PHYSICAL REVIEW D VOLUME 16, NUMBER 6 15 SEPTEMBER 1977

High-energy two-body-to-three-body vector-meson scattering in a Yang-Mills theory

John A. Dickinson
Department of Mathematics, Massachusetts Institute of Technology, Cambridge, Massachusetts 02139
(Received 21 March 1977)

The leading real part of the inelastic two-body-to-three-body scattering amplitude is calculated in the high-energy limit with fixed momentum transfer for vector mesons interacting through a Yang-Mills field. The calculation is carried out to all orders of the coupling constant, and the resulting series is then summed to give a Regge-pole term.

I. INTRODUCTION

The possibility that strong interactions are accurately described by renormalizable non-Abelian gauge field theories has led to a study of their high-energy behavior. Of particular interest is the question of the Reggeization of gauge vector mesons. In 1973, Grisaru, Schnitzer, and Tsao[1] argued that in some models with spontaneously broken vacuum symmetry the necessary criteria for Reggeization are fulfilled. More recently, McCoy and Wu,[2] Lipatov,[3] and Cheng and Lo[4] have separately found that for a Yang-Mills theory with SU(2) symmetry and an isospin-$\frac{1}{2}$ Higgs boson, the sum of the leading terms in the $I=1$ channel (one unit of isospin exchanged) of the elastic scattering amplitude is of the Regge-pole form, corresponding to the Reggeization of the vector meson. It is therefore of interest to determine whether the inelastic amplitudes for this theory also Reggeize. The purpose of this paper is to explicitly demonstrate that, in the leading-logarithm approximation, the high-energy amplitude for two-body-to-three-body scattering is predominantly real and of the Regge-pole form.

The $I=1$ channel of the elastic amplitude is predominantly real and comes from summing over the ladder diagrams. Since the vector meson has spin 1, the asymptotic amplitude for a ladder diagram with n loops is proportional to $g^2 s(g^2 \ln s)^n$. Yet the amplitude for isospin exchange should be much smaller than s. These large terms are canceled when they are summed over all perturbative orders and the resulting amplitude is

$$\frac{2g^2 s(s/\lambda^2)^{-\alpha(t)}}{-t+\lambda^2},$$

where $\alpha(t)>0$ for $t<0$. These same features are also found in production processes: namely, the amplitudes are mainly real, large individual terms are canceled when summed, and the same function $\alpha(t)$ appears as the power of the energy in the Regge-pole terms.

To be specific, consider the scattering processes $V+V\to V+V+A$ in a Yang-Mills SU(2) theory. There are two incoming and two outgoing vector mesons V of high energy and one created particle A of much smaller energy. The created particle is either another vector meson or an isospin-0 scalar. It is assumed that the incoming and outgoing high-energy particles are transversely polarized. To avoid the infrared problem, a complex scalar doublet is introduced and the Higgs mechanism[5] is invoked to give masses to all the vector mesons. In this model, a scalar field with 0 isospin appears after symmetry breaking, and the Higgs and Faddeev-Popov[6] ghosts do not contribute to the leading order.

Let p_1 and p_2 be the four-momenta of the incoming vector mesons, $p_1-\Delta_1, p_2-\Delta_2$ be the momenta of the outgoing vector mesons, and $k=\Delta_1+\Delta_2$ be the momentum of the created particle (see Fig. 1). The kinematic region under consideration is

$$s \gg s_1, s_2 \gg |\Delta_1^2|, |\Delta_2^2|, \lambda^2, M^2,$$

$$g^2 \ln(s/\lambda^2) \sim 1,$$

$$g^2 \ll 1,$$

where $s=(p_1+p_2)^2$, $s_1=(p_1-\Delta_1+k)^2$, and $s_2=(p_2-\Delta_2+k)^2$ are the squares of the energies of various pairs of particles in their center-of-mass systems; $-\Delta_1^2 \approx \vec{\Delta}_{1\perp}^{\,2}$ and $-\Delta_2^2 \approx \vec{\Delta}_{2\perp}^{\,2}$ are the squares of the momentum transfer between incoming and outgoing high-energy particles in the center-of-mass system, with the momenta of the incoming particles pointing in the z direction, and where λ is the vector-meson mass, M is the scalar mass, and g is the coupling constant. It is this region which gives the dominant contribution when calculating the imaginary part of the elastic scattering amplitude by unitarity.

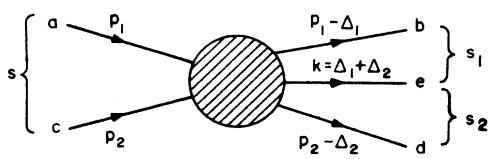

FIG. 1. Schematic diagram of the inelastic scattering process.

The result of the calculation, which agrees with that of Fadin, Kuraev, and Lipatov,[7] is that the amplitude can be written in the Regge-pole form

$$\mathfrak{M} \sim 2g^3 s \frac{1}{(\vec{\Delta}_{1\perp}^{\,2}+\lambda^2)(\vec{\Delta}_{2\perp}^{\,2}+\lambda^2)} \left(\frac{s_1}{\lambda^2}\right)^{-\alpha(\vec{\Delta}_{1\perp})} \times \left(\frac{s_2}{\lambda^2}\right)^{-\alpha(\vec{\Delta}_{2\perp})} \Gamma I \,, \tag{1.1}$$

where

$$\alpha(\vec{\Delta}_\perp) = g^2(\vec{\Delta}_\perp^{\,2}+\lambda^2) \int \frac{d^2\vec{q}_\perp}{(2\pi)^3} \frac{1}{(\vec{q}_\perp^{\,2}+\lambda^2)[(\vec{\Delta}_\perp-\vec{q}_\perp)^2+\lambda^2]} = \frac{g^2}{8\pi^2}(\vec{\Delta}_\perp^{\,2}+\lambda^2)\int_0^1 dx \frac{1}{x(1-x)\vec{\Delta}_\perp^{\,2}+\lambda^2} \,, \tag{1.2}$$

where the vertex function

$$\Gamma = \begin{cases} \vec{\epsilon}_\perp\cdot(\vec{\Delta}_{1\perp}-\vec{\Delta}_{2\perp}) - (p_2\cdot\epsilon)\left(\dfrac{p_1\cdot k}{p_1\cdot p_2} - \dfrac{\vec{\Delta}_{2\perp}^{\,2}+\lambda^2}{p_2\cdot k}\right) + (p_1\cdot\epsilon)\left(\dfrac{p_2\cdot k}{p_1\cdot p_2} - \dfrac{\vec{\Delta}_{1\perp}^{\,2}+\lambda^2}{p_1\cdot k}\right) \\ \quad \text{for vector-meson production with polarization vector } \epsilon \,, & (1.3a) \\ -\lambda \quad \text{for scalar production} \,, & (1.3b) \end{cases}$$

and where the isospin factor

$$I = \begin{cases} i(\delta_{ae}\epsilon_{bcd} - \delta_{be}\epsilon_{acd}) = i(\delta_{de}\epsilon_{abc} - \delta_{ce}\epsilon_{abd}) \quad \text{for vector-meson production} \,, & (1.4a) \\ \delta_{ac}\delta_{bd} - \delta_{ad}\delta_{bc} \quad \text{for scalar production} \,, & (1.4b) \end{cases}$$

where a (= 1, 2, 3) and c (b and d) are the isospin indices for the incoming (outgoing) high-energy particles, and e is the isospin index for the created vector meson. These isospin factors are represented diagrammatically in Fig. 2. Note that the vertex function for vector-meson production (1.3a) is gauge invariant, that is, $\Gamma(\epsilon)|_{\epsilon=k} = 0$.

All $\ln s_1$ and $\ln s_2$ terms come from integrations over the longitudinal momenta. Integrations over transverse momenta may diverge for individual Feynman diagrams, but when the contributions from all diagrams of a given order are added together, the resulting integration is finite. This is shown explicitly through the fifth order and is assumed to be true for higher orders.

The infinite-momentum-space technique[8] is used throughout. For an arbitrary four-vector p define $p_\pm = p_0 \pm p_3$. Then

$$p\cdot q = \tfrac{1}{2}p_+q_- + \tfrac{1}{2}p_-q_+ - \vec{p}_\perp\cdot\vec{q}_\perp \tag{1.5a}$$

and

$$d^4p = \tfrac{1}{2}dp_+dp_-d^2\vec{p}_\perp \,. \tag{1.5b}$$

(The metric is such that $p^2 = p_0^{\,2} - \vec{p}^{\,2}$.) If $p = (p_+, p_-, \vec{p}_\perp)$ then in the center-of-mass system,

FIG. 2. Diagrams with the same isospin factors as the final answer (1.4a) and (1.4b). (a) Vector-meson production. (b) Scalar production.

with the momenta of the incoming particles in the z direction,

$$p_1 = \left(p_{1+}, \frac{\lambda^2}{p_{1+}}, 0\right), \qquad p_2 = \left(\frac{\lambda^2}{p_{2-}}, p_{2-}, 0\right), \tag{1.6}$$

where $p_{1+} = p_{2+} \sim \sqrt{s}$. It further follows that

$$s_1 \sim p_{1+}k_- \,, \quad s_2 \sim p_{2-}k_+ \,, \quad \Delta_{1-} = O\left(\frac{1}{p_{1+}}\right), \quad \Delta_{2+} = O\left(\frac{1}{p_{2-}}\right), \quad \Delta_{1+} \sim k_+ \,, \quad \Delta_{2-} \sim k_- \,, \tag{1.7}$$

and

$$k_+k_- = \vec{k}^2 + \lambda^2 \,.$$

In the center-of-mass system the vertex function Γ for vector-meson production (1.3a) can be written

$$\Gamma = \vec{\epsilon}_\perp\cdot(\vec{\Delta}_{1\perp}-\vec{\Delta}_{2\perp}) - \epsilon_+k_-\left(\frac{1}{2} - \frac{\vec{\Delta}_{2\perp}^{\,2}+\lambda^2}{\vec{k}_\perp^{\,2}+\lambda^2}\right) + \epsilon_-k_+\left(\frac{1}{2} - \frac{\vec{\Delta}_{1\perp}^{\,2}+\lambda^2}{\vec{k}_\perp^{\,2}+\lambda^2}\right). \tag{1.8}$$

The relevant Feynman rules[9] are (i) an overall factor of $-i$, (ii) a factor of $-i$ for each vertex, (iii) $-i\delta_{ab}g_{\mu\nu}/(k^2-\lambda^2+i\epsilon)$ for the vector-meson

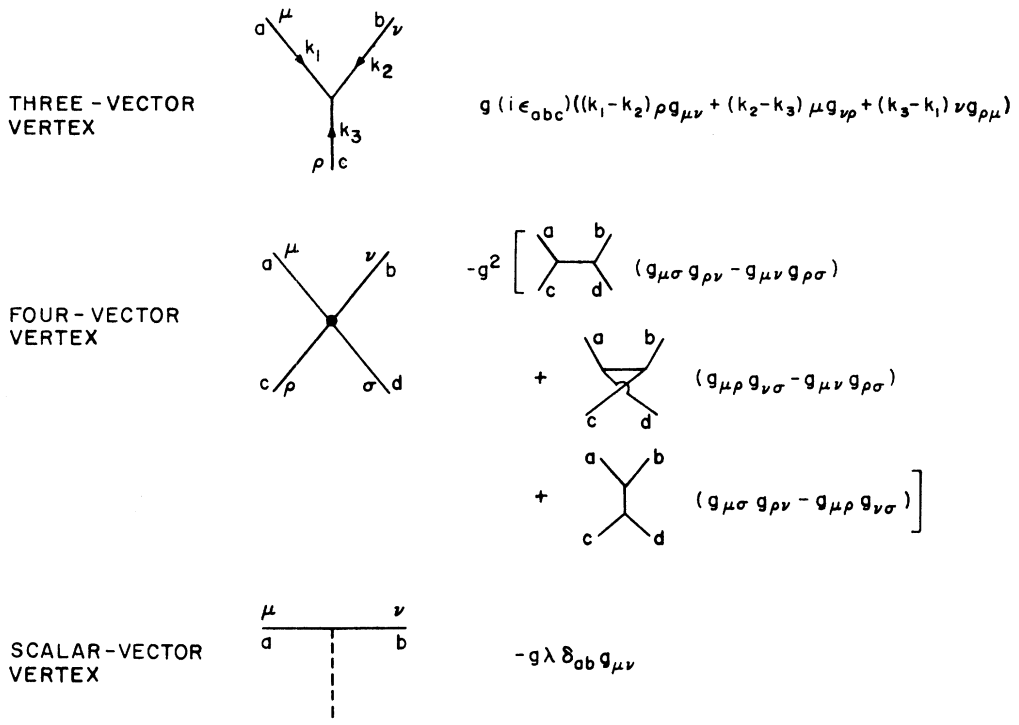

FIG. 3. The Feynman rules for the vertices. The solid lines are vector mesons and the dashed line is the scalar. For the four-vector vertex, the isospin factors are given diagrammatically, with each of the diagrams standing for the isospin factor associated with it.

propagator (here a and b are the isospin indices and μ and ν are the space-time indices), (iv) $i/(k^2-M^2+i\epsilon)$ for the scalar propagator, (v) $g(i\epsilon_{abc})((k_1-k_2)_\rho g_{\mu\nu}+(k_2-k_3)_\mu g_{\nu\rho}+(k_3-k_1)_\nu g_{\rho\mu})$ for a three-vector vertex, (vi)

$$-g^2[(i\epsilon_{eca})(i\epsilon_{ebd})(g_{\mu\sigma}g_{\rho\nu}-g_{\mu\nu}g_{\rho\sigma})$$
$$+(i\epsilon_{eda})(i\epsilon_{ebc})(g_{\mu\rho}g_{\nu\sigma}-g_{\mu\nu}g_{\rho\sigma})$$
$$+(i\epsilon_{eab})(i\epsilon_{edc})(g_{\mu\sigma}g_{\rho\nu}-g_{\mu\rho}g_{\nu\sigma})]$$

for a four-vector vertex, and (vii) $-g\lambda\delta_{ab}g_{\mu\nu}$ for a scalar-vector vertex. The vertex factors are illustrated in Fig. 3. Note that the four-vector vertex consists of three terms, corresponding to the three ways it can be "unfused" to make two three-vector vertices.

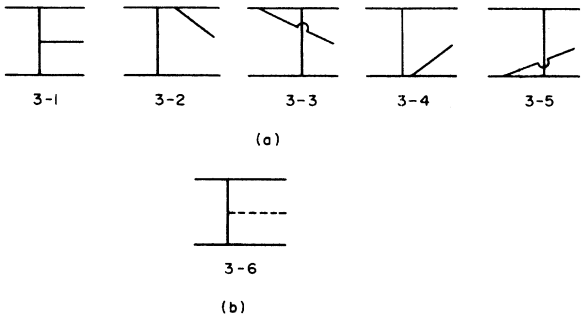

FIG. 4. The third-order Feynman diagrams which contribute in the high-energy limit to (a) vector-meson production (five diagrams) and (b) scalar production (one diagram).

II. THE THIRD-ORDER CALCULATION

Five diagrams contribute to the third-order amplitude for vector-meson production when the high-momentum particles are transversely polarized. They are shown in Fig. 4. Each amplitude $\mathfrak{M}$ can be written as the product of isospin factors I ($i\epsilon_{abc}$ for each three-vector vertex; δ_{ab} for each scalar-vector vertex) and nonisospin or space-time factors M, $\mathfrak{M}=M\cdot I$. The space-time amplitude for diagram 3-1 (shown in Fig. 5) equals

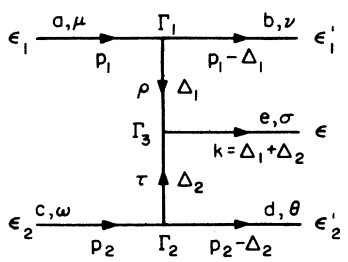

FIG. 5. Feynman diagram 3-1.

$$M_1^{(3)} = (-i)^{1+3+2} g^3 \epsilon_{1\mu} \epsilon_{1'\nu} \epsilon_{2\omega} \epsilon_{2'\theta} \epsilon_{\sigma} \Gamma_1 \Gamma_2 \Gamma_3 \times (\Delta_1^2 - \lambda^2 + i\epsilon)^{-1} (\Delta_2^2 - \lambda^2 + i\epsilon)^{-1}, \quad (2.1)$$

where

$$\Gamma_1 = (2p_1 - \Delta_1)_\rho g_{\mu\nu} + (-p_1 + 2\Delta_1)_\mu g_{\nu\rho} + (-p_1 - \Delta_1)_\nu g_{\rho\mu}, \quad (2.2)$$

$$\Gamma_2 = (p_2 + \Delta_2)_\theta g_{\omega\tau} + (p_2 - 2\Delta_2)_\omega g_{\tau\theta} + (-2p_2 + \Delta_2)_\tau g_{\theta\omega}, \quad (2.3)$$

and

$$\Gamma_3 = (2\Delta_1 + \Delta_2)_\tau g_{\rho\sigma} + (-\Delta_1 - 2\Delta_2)_\rho g_{\sigma\tau} + (\Delta_2 - \Delta_1)_\sigma g_{\rho\tau}. \quad (2.4)$$

The high-energy amplitude must be proportional to $s \sim 2p_1 \cdot p_2$. Since ϵ_1 and $\epsilon_{1'}$ are transverse,

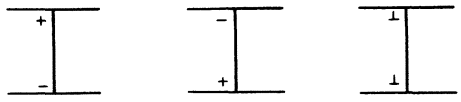

FIG. 6. The three possible polarizations of a line in a Feynman diagram.

their components are of order unity; hence the only p_1 dependence in the amplitude comes from the vertex Γ_1. Since $\epsilon_1 \cdot p_1 = \epsilon_{1'} \cdot (p_1 - \Delta_1) = 0$, it follows that $\epsilon_{1\mu}(-p_1 + 2\Delta_1)_\mu = 2\epsilon_1 \cdot \Delta_1$ and $\epsilon_{1'\nu}(-p_1 - \Delta_1)_\nu = -2\epsilon_{1'} \cdot \Delta_1$ and so these terms are independent of p_1. Therefore the $(-p_1 + 2\Delta_1)_\mu$ and $(-p_1 - \Delta_1)_\nu$ terms in Γ_1 do not contribute and will be dropped. Likewise the $(p_2 + \Delta_2)_\theta$ and $(p_2 - 2\Delta_2)_\omega$ terms are dropped from Γ_2. Then the numerator of (2.1) is proportional to

$$\begin{aligned}(2p_1 - \Delta_1)_\rho (-2p_2 + \Delta_2)_\tau \Gamma_3 \epsilon_\sigma &= (-2p_2 + \Delta_2) \cdot (2\Delta_1 + \Delta_2)\epsilon \cdot (2p_1 - \Delta_1) + (2p_1 - \Delta_1) \cdot (-\Delta_1 - 2\Delta_2)\epsilon \cdot (-2p_2 + \Delta_2) \\ &\quad + \epsilon \cdot (\Delta_2 - \Delta_1)(2p_1 - \Delta_1) \cdot (-2p_2 + \Delta_2) \\ &\sim -2p_{1+}p_{2-}\epsilon_- k_+ + 2p_{1+}p_{2-}\epsilon_+ k_- - 2p_{1+}p_{2-}(\tfrac{1}{2}\epsilon_+ k_- - \tfrac{1}{2}\epsilon_- k_+ - \vec{\epsilon}_\perp \cdot (\vec{\Delta}_{2\perp} - \vec{\Delta}_{1\perp})) \\ &= -2p_{1+}p_{2-}((\vec{\Delta}_{1\perp} - \vec{\Delta}_{2\perp}) \cdot \vec{\epsilon}_\perp - \tfrac{1}{2}\epsilon_+ k_- + \tfrac{1}{2}\epsilon_- k_+). \end{aligned} \quad (2.5)$$

Since $\Delta_1^2 = \Delta_{1+}\Delta_{1-} - \vec{\Delta}_{1\perp}^2 \sim -\vec{\Delta}_{1\perp}^2$ and likewise $\Delta_2^2 \sim -\vec{\Delta}_{2\perp}^2$ and since $\epsilon_{1\mu}\epsilon_{1'\nu}g_{\mu\nu} = -\vec{\epsilon}_{1\perp} \cdot \vec{\epsilon}_{1'\perp}$, etc., the amplitude is

$$M_1^{(3)} \sim 2g^3 s (\vec{\epsilon}_{1\perp} \cdot \vec{\epsilon}_{1'\perp})(\vec{\epsilon}_{2\perp} \cdot \vec{\epsilon}_{2'\perp}) \frac{1}{(\vec{\Delta}_{1\perp}^2 + \lambda^2)(\vec{\Delta}_{2\perp}^2 + \lambda^2)} (\vec{\epsilon}_\perp \cdot (\vec{\Delta}_{1\perp} - \vec{\Delta}_{2\perp}) - \tfrac{1}{2}\epsilon_+ k_- + \tfrac{1}{2}\epsilon_- k_+). \quad (2.6)$$

In the high-energy limit it is simpler to calculate this and all other diagrams using the $(+, -, \perp)$ notation throughout. In the product $p_\mu q_\mu$ the sum over the four space-time indices can be replaced by the sum of the three terms on the right-hand side of (1.5a). This is represented diagrammatically by notating each line of a Feynman diagram with one of the pairs $(+, -)$, $(-, +)$, or $(\perp, \perp)$, with one sign near each of the two end points of the line, as shown in Fig. 6. Each line can have any of these three polarizations, and all possibilities for all internal lines are summed over. Each three-point vertex then has three signs associated with it, one corresponding to each line. Since a + component always multiplies a − component and a $\perp$ component always multiplies a $\perp$ component,

$$g_{++} = g_{--} = g_{\perp+} = g_{+\perp} = g_{\perp-} = g_{-\perp} = 0. \quad (2.7)$$

With the convention that a longitudinal (i.e., + or −) component is always multiplied by an extra factor of $1/\sqrt{2}$,

$$g_{+-} = g_{-+} = 1 \text{ and } g_{\perp\perp} = -1, \quad (2.8)$$

so that the product of two longitudinal components will reproduce the factor of $\frac{1}{2}$ in (1.5a) and the product of two transverse components will reproduce the factor of −1 in (1.5a). The advantage of this technique is that all lines emerging from high-momentum lines[10] are longitudinally polarized; further, if the line emerges from a large + (−) momentum line, then the sign on the emerging line associated with that vertex is + (−). This is equivalent to the approximation of dropping all those terms in a vertex on a large momentum line which do not give a contribution proportional to that large momentum. This was illustrated above in dropping the $(-p_1 + 2\Delta_1)_\mu$ and $(-p_1 - \Delta_1)_\nu$ terms from Γ_1. Using this method, (2.2) and (2.3) become, respectively,

$$\Gamma_1 \sim \frac{2p_{1+}}{\sqrt{2}} \quad \text{and} \quad \Gamma_2 \sim -\frac{2p_{2-}}{\sqrt{2}}, \quad (2.9)$$

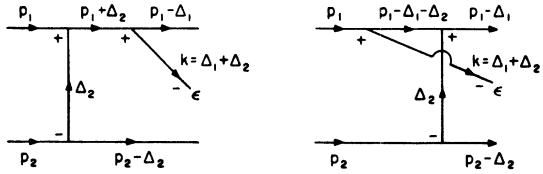

FIG. 7. (a) Feynman diagram 3-2. (b) Feynman diagram 3-3.

so that $\Gamma_1\Gamma_2 \sim -2s$.

Feynman diagram 3-2 is shown in Fig. 7(a). The space-time amplitude is

$$M_2^{(3)} \sim (-i)^{1+3+2} g^3 \left(\frac{2p_{1+}}{\sqrt{2}}\right)^2 \left(\frac{-2p_{2-}}{\sqrt{2}}\right) (\Delta_2{}^2 - \lambda^2 + i\epsilon)^{-1} \times [(p_1+\Delta_2)^2 - \lambda^2 + i\epsilon]^{-1} \frac{\epsilon_-}{\sqrt{2}} \sim -2g^3 p_{1+}p_{2-} \frac{\epsilon_-}{k_-} \frac{1}{\vec{\Delta}_{2\perp}{}^2 + \lambda^2} . \quad (2.10)$$

[Since the polarization factors $(\vec{\epsilon}_{1\perp}\cdot\vec{\epsilon}_{1'\perp})(\vec{\epsilon}_{2\perp}\cdot\vec{\epsilon}_{2'\perp})$ are common to all the amplitudes calculated in this paper, they will henceforth be suppressed.]

Feynman diagram 3-3 is shown in Fig. 7(b). The only difference between its amplitude and that of diagram 3-2 is that the propagator $(p_1-\Delta_1-\Delta_2)^2 - \lambda^2 + i\epsilon$ replaces $(p_1+\Delta_2)^2 - \lambda^2 + i\epsilon$. Since $(p_1-\Delta_1-\Delta_2)^2 - \lambda^2 + i\epsilon \sim -p_{1+}k_-$, the space-time amplitude $M_3^{(3)} \sim -M_2^{(3)}$. The diagrams do not cancel, however, because they have different isospin factors. This will be discussed below.

Diagram 3-4 (3-5) is obtained from diagram 3-2 (3-3) by reflecting through a horizontal plane mirror, under which

$$p_1 \leftrightarrow p_2, \quad \Delta_1 \leftrightarrow \Delta_2, \quad + \leftrightarrow - . \quad (2.11)$$

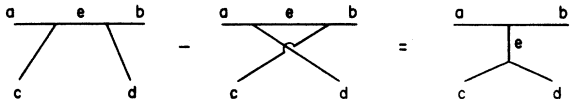

FIG. 8. The Jacobi identity expressed diagrammatically. Each diagram stands for the isospin factor associated with it.

Under this reversal, each vector-meson vertex, which was previously calculated from the Feynman rules by tracing the incoming momentum in a clockwise fashion, is now traced counterclockwise; this introduces a factor of (-1) to revert to the correct, clockwise, ordering. Thus

$$M_4^{(3)}(p_{1+}, p_{2-}, k_+, k_-, \vec{\Delta}_{1\perp}, \vec{\Delta}_{2\perp}, \epsilon_+, \epsilon_-, \epsilon_\perp) \sim (-1)^3 M_2^{(3)}(p_{2-}, p_{1+}, k_-, k_+, \vec{\Delta}_{2\perp}, \vec{\Delta}_{1\perp}, \epsilon_-, \epsilon_+, \epsilon_\perp) \sim 2g^3 p_{1+}p_{2-} \frac{\epsilon_+}{k_+} \frac{1}{\vec{\Delta}_{1\perp}{}^2 + \lambda^2} . \quad (2.12)$$

Likewise

$$M_5^{(3)} \sim -2g^3 p_{1+}p_{2-} \frac{\epsilon_+}{k_+} \frac{1}{\vec{\Delta}_{1\perp}{}^2 + \lambda^2} . \quad (2.13)$$

The Jacobi identity for isospin,[11]

$$(i\epsilon_{eca})(i\epsilon_{ebd}) - (i\epsilon_{eda})(i\epsilon_{ebc}) = (i\epsilon_{eab})(i\epsilon_{edc}) , \quad (2.14)$$

is expressed diagrammatically in Fig. 8. If I is the isospin factor for a given diagram, it implies that

$$I_2^{(3)} - I_3^{(3)} = I_1^{(3)} \quad \text{and} \quad I_4^{(3)} - I_5^{(3)} = I_1^{(3)} . \quad (2.15)$$

Therefore, the total space-time amplitude for the third order is

$$M^{(3)} = M_1^{(3)} + M_2^{(3)} + M_4^{(3)} \sim 2g^3 s \frac{1}{(\vec{\Delta}_{1\perp}{}^2 + \lambda^2)(\vec{\Delta}_{2\perp}{}^2 + \lambda^2)} \left[\vec{\epsilon}_\perp \cdot (\vec{\Delta}_{1\perp} - \vec{\Delta}_{2\perp}) - \epsilon_+ k_- \left(\frac{1}{2} - \frac{\vec{\Delta}_{2\perp}{}^2 + \lambda^2}{\vec{k}_\perp{}^2 + \lambda^2}\right) + \epsilon_- k_+ \left(\frac{1}{2} - \frac{\vec{\Delta}_{1\perp}{}^2 + \lambda^2}{\vec{k}_\perp{}^2 + \lambda^2}\right)\right] \quad (2.16)$$

and the isospin is that of the diagram in Fig. 2(a).

For scalar production, only diagram 3-6, shown in Fig. 4(b), contributes. A simple calculation shows that its amplitude is

$$M_S^{(3)} \sim -2g^3 \lambda s \frac{1}{(\vec{\Delta}_{1\perp}{}^2 + \lambda^2)(\vec{\Delta}_{2\perp}{}^2 + \lambda^2)} , \quad (2.17)$$

with isospin of the diagram in Fig. 2(b).

III. THE FIFTH-ORDER CALCULATION

Thirty six fifth-order Feynman diagrams for vector-meson production are shown in Fig. 9. No other diagrams contribute to the high-energy limit. Diagram 5-1, shown in Fig. 10, has the space-time amplitude

$$M_1^{(5)} \sim (-i)^{1+5+5} g^5 \left(\frac{2p_{1+}}{\sqrt{2}}\right)^2 \left(\frac{-2p_{2-}}{\sqrt{2}}\right) \frac{-1}{\vec{\Delta}_{2\perp}^{\,2}+\lambda^2} \frac{1}{2} \int \frac{d^2\vec{q}_\perp}{(2\pi)^4} \int dq_- \int dq_+ \frac{\Gamma_1\Gamma_2}{D_1} , \tag{3.1}$$

where

$$\Gamma_1\Gamma_2 \sim \frac{1}{\sqrt{2}} \left(-\vec{\epsilon}_\perp \cdot (\vec{\Delta}_{2\perp} + \vec{q}_\perp)(-2k_- + q_-) - \vec{\epsilon}_\perp \cdot (\vec{\Delta}_{2\perp} - \vec{\Delta}_{1\perp} - 2\vec{q}_\perp)(-k_- + 2q_-) + \tfrac{1}{2}\epsilon_+(-k_- + 2q_-)(-k_- - q_-) \right.$$
$$\left. - \epsilon_-(\vec{\Delta}_{2\perp} + \vec{q}_\perp) \cdot (\vec{q}_\perp + 2\vec{\Delta}_{1\perp} + \vec{\Delta}_{2\perp}) + \tfrac{1}{2}\epsilon_-(-q_+)(-k_- + 2q_-) + \tfrac{1}{2}\epsilon_-(-k_- + 2q_-)(k_+ - q_+) \right) \tag{3.2}$$

and

$$D_1 = ((p_1+q)^2 - \lambda^2 + i\epsilon)((q+\Delta_1)^2 - \lambda^2 + i\epsilon)((\Delta_2 - q)^2 - \lambda^2 + i\epsilon)(q^2 - \lambda^2 + i\epsilon)$$
$$\sim ((p_{1+}+q_+)q_- - \vec{q}_\perp^{\,2} - \lambda^2 + i\epsilon)((q_+ + \Delta_{1+})q_- - (\vec{q}_\perp + \vec{\Delta}_{1\perp})^2 - \lambda^2 + i\epsilon)$$
$$\times ((q_- - \Delta_{2-})q_+ - (\vec{\Delta}_{2\perp} - \vec{q}_\perp)^2 - \lambda^2 + i\epsilon)(q_+q_- - \vec{q}_\perp^{\,2} - \lambda^2 + i\epsilon) . \tag{3.3}$$

After this approximation of D_1, the q_+ integral is evaluated by contour integration. The zeros of (3.3) occur at

$$q_+ = -p_{1+} + \frac{1}{q_-}(\vec{q}_\perp^{\,2} + \lambda^2 - i\epsilon) , \tag{3.4a}$$

$$q_+ = -\Delta_{1+} + \frac{1}{q_-}((\vec{q}_\perp + \vec{\Delta}_{1\perp})^2 + \lambda^2 - i\epsilon) , \tag{3.4b}$$

$$q_+ = \frac{-1}{\Delta_{2-} - q_-}((\vec{\Delta}_{2\perp} - q_\perp)^2 + \lambda^2 - i\epsilon) , \tag{3.4c}$$

and

$$q_+ = \frac{1}{q_-}(\vec{q}_\perp^{\,2} + \lambda^2 - i\epsilon) . \tag{3.4d}$$

If $q_- < 0$, then all these poles of the integrand are in the upper half of the complex q_+ plane, and the contour may be closed in the lower half-plane to give zero. Similarly, if $q_- > \Delta_{2-}$, all the poles are again zero. Thus the only nonzero contribution

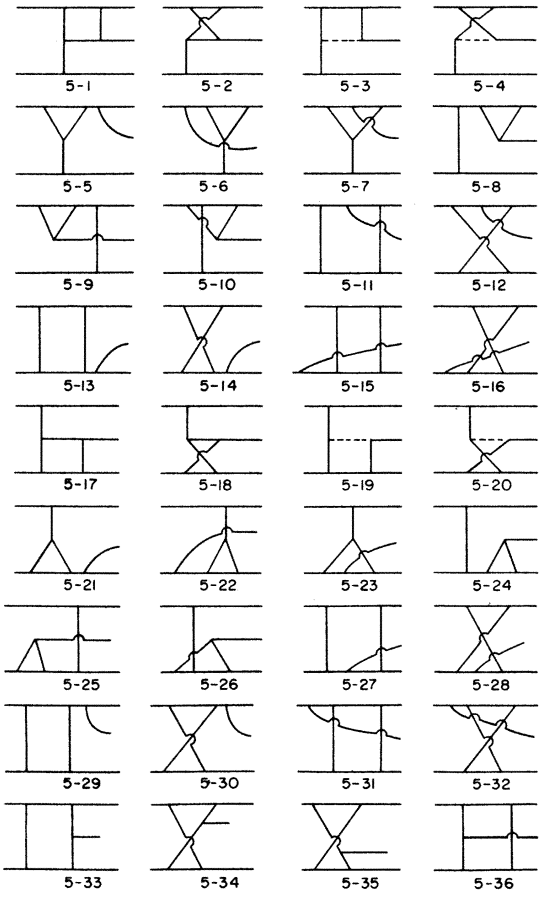

FIG. 9. Fifth-order Feynman diagrams for vector-meson production.

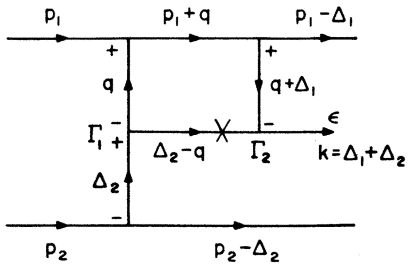

FIG. 10. Feynman diagram 5-1. The cross (×) indicates the pole in the complex q_+ plane about which the contour is closed.

comes from the region[12]

$$0<q_-<\Delta_{2-}\ . \tag{3.5}$$

[Actually, in approximating $(p_1+q)^2$ by $(p_{1+}+q_+)q_- - \vec{q}_\perp^{\,2}$ in (3.3), it was tacitly assumed that $q_- \gg p_{1-} = \lambda^2/p_{1+}$.] In this region, the contour is closed about the only pole in the upper half-plane, namely (3.4c). This is indicated in Fig. 10 by a cross (×) on the line carrying momentum $\Delta_2 - q$.

Therefore

$$\int dq_- \int dq_+ \frac{\Gamma_1\Gamma_2}{D_1} \sim \int dq_- \Gamma_1\Gamma_2 \frac{-2\pi i}{\Delta_{2-}-q_-} \frac{1}{p_{1+}q_- - \left[q_-\left(k_+ - \frac{(\vec{\Delta}_{2\perp}-\vec{q}_\perp)^2+\lambda^2}{\Delta_{2-}-q_-}\right) - (\vec{q}_\perp+\vec{\Delta}_{1\perp})^2 - \lambda^2 + i\epsilon\right]^{-1}}$$
$$\times\left[\frac{-q_-}{\Delta_{2-}-q_-}((\vec{\Delta}_{2\perp}-\vec{q}_\perp)^2+\lambda^2) - \vec{q}_\perp^{\,2} - \lambda^2 + i\epsilon\right]^{-1}, \tag{3.6}$$

where the q_+ terms appearing in $\Gamma_1\Gamma_2$ are replaced by (3.4c). The only region in this integration which contributes to $\ln(s_1/\lambda^2)$ is

$$\frac{\lambda^2}{p_{1+}} \ll q_- \ll k_-\ , \tag{3.7}$$

so that

$$q_-k_+ \ll 1\ ,$$
$$q_+ \sim -\frac{(\vec{\Delta}_{2\perp}-\vec{q}_\perp)^2+\lambda^2}{k_-}\ , \tag{3.8}$$
and
$$q_-q_+ \ll 1\ .$$

Then

$$\Gamma_1\Gamma_2 \sim \frac{k_-}{\sqrt{2}}\Big[2\vec{\epsilon}_\perp\cdot(\vec{\Delta}_{2\perp}+\vec{q}_\perp) + \vec{\epsilon}_\perp\cdot(\vec{\Delta}_{2\perp}-\vec{\Delta}_{1\perp}-2\vec{q}_\perp) + \tfrac{1}{2}\epsilon_+k_- + \frac{\epsilon_-}{k_-}(-(\vec{\Delta}_{2\perp}+\vec{q}_\perp)\cdot(\vec{q}_\perp+2\vec{\Delta}_{1\perp}+\vec{\Delta}_{2\perp})$$
$$-((\vec{\Delta}_{2\perp}-\vec{q}_\perp)^2+\lambda^2) - \tfrac{1}{2}(\vec{k}_\perp^{\,2}+\lambda^2))\Big]$$
$$= \frac{k_-}{\sqrt{2}}\Big[\vec{\epsilon}_\perp\cdot(3\vec{\Delta}_{2\perp}-\vec{\Delta}_{1\perp}) + \tfrac{1}{2}\epsilon_+k_- + \frac{\epsilon_-}{k_-}(-\tfrac{3}{2}(\vec{k}_\perp^{\,2}+\lambda^2) + 2(\vec{\Delta}_{1\perp}^{\,2}+\lambda^2) - (\vec{\Delta}_{2\perp}^{\,2}+\lambda^2)$$
$$-(\vec{q}_\perp^{\,2}+\lambda^2) - ((\vec{\Delta}_{1\perp}+\vec{q}_\perp)^2+\lambda^2)+\lambda^2)\Big]\ , \tag{3.9}$$

where the ϵ_- component has been expressed in terms of the two denominator factors $\vec{q}_\perp^{\,2}+\lambda^2$ and $(\vec{\Delta}_{1\perp}+\vec{q}_\perp)^2+\lambda^2$ and $\vec{\Delta}_{1\perp}^{\,2}+\lambda^2$, $\vec{\Delta}_{2\perp}^{\,2}+\lambda^2$, $\vec{k}_\perp^{\,2}+\lambda^2$.

Using the approximations (3.8), the only q_- dependence in $M_1^{(5)}$ is from D_1, so the q_- integration becomes

$$\int_{\lambda^2/p_{1+}}^{k_-} dq_- \frac{1}{q_-} = \ln\left(\frac{p_{1+}k_-}{\lambda^2}\right) \sim \ln\left(\frac{s_1}{\lambda^2}\right)\ . \tag{3.10}$$

Thus

$$M_1^{(5)} \sim g^5 s \ln\left(\frac{s_1}{\lambda^2}\right) \frac{1}{\vec{\Delta}_{2\perp}^{\,2}+\lambda^2} \int \frac{d^2\vec{q}_\perp}{(2\pi)^3} \frac{1}{(\vec{q}_\perp^{\,2}+\lambda^2)[(\vec{q}_\perp+\vec{\Delta}_{1\perp})^2+\lambda^2]}$$
$$\times\left(\vec{\epsilon}_\perp\cdot(3\vec{\Delta}_{2\perp}-\vec{\Delta}_{1\perp}) + \tfrac{1}{2}\epsilon_+k_- + \frac{\epsilon_-}{k_-}(-\tfrac{3}{2}(\vec{k}_\perp^{\,2}+\lambda^2) + 2(\vec{\Delta}_{1\perp}^{\,2}+\lambda^2) - (\vec{\Delta}_{2\perp}^{\,2}+\lambda^2)+\lambda^2)\right)$$
$$-2g^5 s \ln\left(\frac{s_1}{\lambda^2}\right) \frac{1}{\vec{\Delta}_{2\perp}^{\,2}+\lambda^2} \frac{\epsilon_-}{k_-} \int \frac{d^2\vec{q}_\perp}{(2\pi)^3} \frac{1}{\vec{q}_\perp^{\,2}+\lambda^2}\ , \tag{3.11}$$

where the origin of the logarithmically divergent integral has been shifted. Thus the integration over the transverse momentum $\vec{q}_\perp$ does not converge. This divergence will cancel out exactly when contributions from all diagrams are added together.

Feynman diagram 5-2 is shown in Fig. 11. It differs from diagram 5-1 by the replacement of the propagator $(p_1+q)^2-\lambda^2+i\epsilon$ by $(p_1-q-\Delta_1)^2-\lambda^2+i\epsilon$. Since

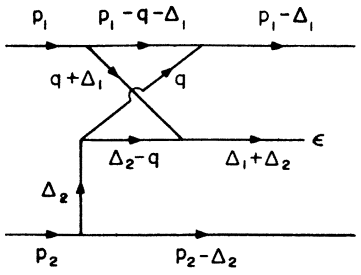

FIG. 11. Feynman diagram 5-2.

$$(p_1+q)^2-\lambda^2+i\epsilon \sim p_{1+}q_- \tag{3.12a}$$

and

$$(p_1-q-\Delta_1)^2-\lambda^2+i\epsilon \sim -p_{1+}q_- \ , \tag{3.12b}$$

it follows that $M_2^{(5)} \sim -M_1^{(5)}$. An application of the Jacobi identity for isospin [see (2.14) and Fig. 8] and the use of $(i\epsilon_{dae})(i\epsilon_{dfb})(i\epsilon_{fec}) = i\epsilon_{acb}$ (illustrated in Fig. 12), shows that $I_1^{(5)} - I_2^{(5)} = I_1^{(3)}$, as seen in Fig. 13. Thus,

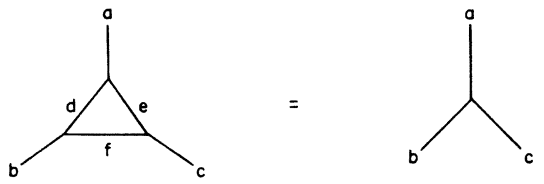

FIG. 12. The diagrammatic expression of the isospin identity $(i\epsilon_{dae})(i\epsilon_{dfb})(i\epsilon_{fec}) = i\epsilon_{acb}$.

$$\mathfrak{M}_1^{(5)} + \mathfrak{M}_2^{(5)} = M_1^{(5)} I_1^{(5)} + M_2^{(5)} I_2^{(5)} \sim M_1^{(5)} I_1^{(3)} \ . \tag{3.13}$$

The space-time amplitude of Feynman diagram 5-3 (shown in Fig. 14) differs from that of diagram 5-1 in two respects: First, the vector-meson propagator $-i/[(\Delta_2-q)^2-\lambda^2+i\epsilon]$ is replaced by the scalar propagator $i/[(\Delta_2-q)^2-M^2+i\epsilon]$, and so (3.4c) is replaced by $q_+ = [-1/(\Delta_{2-}-q_-)]((\vec{\Delta}_{2\perp}-\vec{q}_\perp)^2-M^2+i\epsilon)$, and second, $\Gamma_1\Gamma_2$ is replaced by $(-\lambda)^2\epsilon_-/\sqrt{2}$. Thus

$$M_3^{(5)} \sim -\lambda^2 g^5 s \ln\left(\frac{s_1}{\lambda^2}\right) \frac{1}{\vec{\Delta}_{2\perp}^{\,2}+\lambda^2} \frac{\epsilon_-}{k_-} \int \frac{d^2\vec{q}_\perp}{(2\pi)^3} \frac{1}{(\vec{q}_\perp^{\,2}+\lambda^2)[(\vec{q}_\perp+\vec{\Delta}_{1\perp})^2+\lambda^2]} \ . \tag{3.14}$$

By (3.12), $M_4^{(5)} \sim -M_3^{(5)}$. Since $I_3^{(5)} = I_2^{(3)}$ and $I_4^{(5)} = I_3^{(3)}$, using (2.15),

$$\mathfrak{M}_3^{(5)} + \mathfrak{M}_4^{(5)} = M_3^{(5)} I_3^{(5)} + M_4^{(5)} I_4^{(5)} \sim M_3^{(5)} I_1^{(3)} \ . \tag{3.15}$$

Feynman diagram 5-5 is shown in Fig. 15. Its space-time amplitude is

$$M_5^{(5)} \sim \tfrac{1}{2}(-i)^{11} g^5 \left(\frac{2p_{1+}}{\sqrt{2}}\right)^3 \left(\frac{-2p_{2-}}{\sqrt{2}}\right) \frac{-1}{\vec{\Delta}_{2\perp}^{\,2}+\lambda^2} \frac{1}{p_{1+}k_-} \int \frac{d^2\vec{q}_\perp}{(2\pi)^4} \int dq_- \int dq_+ \frac{\frac{1}{2}(2q_- - k_-)\epsilon_-}{D_5} \ , \tag{3.16}$$

where

$$D_5 \sim p_{1+}q_-(q_+q_- - \vec{q}_\perp^{\,2} - \lambda^2 + i\epsilon)(-q_+(\Delta_{2-}-q_-) - (\vec{\Delta}_{2\perp}-\vec{q}_\perp)^2 - \lambda^2 + i\epsilon) \ . \tag{3.17}$$

The q_+ integration is zero unless (3.5) holds and in this case the contour is closed in the upper half-plane about the pole at

$$q_+ = -\frac{(\vec{\Delta}_{2\perp}-\vec{q}_\perp)^2+\lambda^2-i\epsilon}{\Delta_{2-}-q_-} \ . \tag{3.18}$$

So

$$\int dq_- \int dq_+ \frac{2q_- - k_-}{D_5} \sim (-2\pi i) \int dq_- \frac{2q_- - k_-}{p_{1+}q_-(k_- - q_-)\{-q_-[(\vec{\Delta}_{2\perp}-\vec{q}_\perp)^2+\lambda^2]/(k_- - q_-) - \vec{q}_\perp^{\,2} - \lambda^2 + i\epsilon\}} \ , \tag{3.19}$$

and the dominant contribution to this integral again comes from the region (3.7), where it is approximately

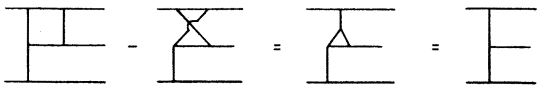

FIG. 13. Diagrammatic calculation of the isospin associated with the combined amplitude of Feynman diagrams 5-1 and 5-2.

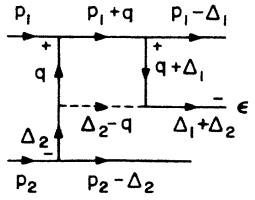

FIG. 14. Feynman diagram 5-3.

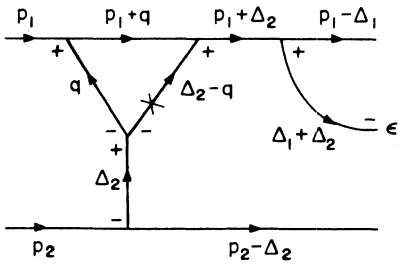

FIG. 15. Feynman diagram 5-5.

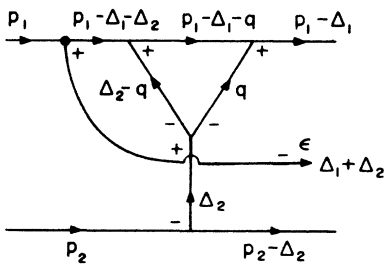

FIG. 16. Feynman diagram 5-6.

$$-2\pi i\,\frac{1}{p_{1+}}\,\frac{1}{\vec{q}_\perp^{\,2}+\lambda^2}\int_{\lambda^2/p_{1+}}^{k_-}\frac{dq_-}{q_-}\sim -2\pi i\,\frac{1}{p_{1+}}\,\frac{1}{\vec{q}_\perp^{\,2}+\lambda^2}\ln\left(\frac{s_1}{\lambda^2}\right)\quad . \tag{3.20}$$

Therefore,

$$M_5^{(5)}\sim g^5 s\ln\left(\frac{s_1}{\lambda^2}\right)\frac{1}{\vec{\Delta}_{2\perp}^{\,2}+\lambda^2}\,\frac{\epsilon_-}{k_-}\int\frac{d^2\vec{q}_\perp}{(2\pi)^3}\,\frac{1}{\vec{q}_\perp^{\,2}+\lambda^2}\quad , \tag{3.21}$$

which is divergent in the transverse-momentum integration.

Feynman diagram 5-6, shown in Fig. 16, differs from Feynman diagram 5-5 by the replacement of $p_1+\Delta_2$ by $p_1-\Delta_1-\Delta_2$, the replacement of p_1+q by $p_1-q-\Delta_1$, and in the ordering of the internal vertex (the one off the large momentum lines). Since

$$[(p_1+\Delta_2)^2-\lambda^2+i\epsilon][(p_1+q)^2-\lambda^2+i\epsilon]\sim[(p_1-\Delta_1-\Delta_2)^2-\lambda^2+i\epsilon][(p_1-q-\Delta_1)^2-\lambda^2+i\epsilon]\sim p_{1+}{}^2q_-k_-\quad , \tag{3.22}$$

the replacement of the propagators makes no change in the asymptotic form of the amplitude. However, in diagram 5-5, the clockwise ordering of the momenta into the internal vertex is $(\Delta_2, -q, q-\Delta_2)$, whereas the ordering for diagram 5-6 is $(\Delta_2, q-\Delta_2, -q)$. According to the Feynman rules for a three-vector vertex (Fig. 3), this introduces a difference of a minus sign, so that $M_6^{(5)}\sim -M_5^{(5)}$. Using the isospin identity of Fig. 12, $I_5^{(5)}=I_2^{(3)}$ and $I_6^{(5)}=I_3^{(3)}$, so from (2.15)

$$\mathfrak{M}_5^{(5)}+\mathfrak{M}_6^{(5)}=M_5^{(5)}I_1^{(3)}\quad . \tag{3.23}$$

Feynman diagram 5-7 is shown with two different internal momentum flows in Figs. 17(a) and 17(b). By a now familiar analysis, the two diagrams differ only in two propagators on the large + momentum line and in the ordering of the internal vertex. Each of these three differences causes a change of a minus sign; so

$$M_7^{(5)}\sim(-1)^3M_7^{(5)}\sim 0 \tag{3.24}$$

to leading order. Thus this diagram does not contribute.[13]

The space-time amplitude for Feynman diagram 5-8, drawn in Fig. 18(a), is

$$M_8^{(5)}\sim\tfrac{1}{2}(-i)^{11}g^5\left(\frac{2p_{1+}}{\sqrt{2}}\right)^3\left(\frac{-2p_{2-}}{\sqrt{2}}\right)\frac{-1}{\vec{\Delta}_{2\perp}^{\,2}+\lambda^2}\,\frac{1}{p_{1+}k_-}\int\frac{d^2\vec{q}}{(2\pi)^4}\int dq_-\int dq_+$$
$$\times\frac{\tfrac{1}{2}(2q_--k_-)\epsilon_-}{p_{1+}q_-(-q_+(\Delta_{2-}-q_-)-(\vec{\Delta}_{2\perp}-\vec{q}_\perp)^2-\lambda^2+i\epsilon)((q_++k_+)q_--(\vec{q}_\perp+\vec{\Delta}_{1\perp})^2-\lambda^2+i\epsilon)}\quad . \tag{3.25}$$

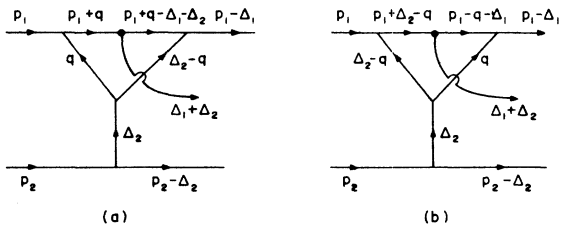

FIG. 17. A diagrammatic argument that Feynman diagram 5-7 does not contribute to leading order.

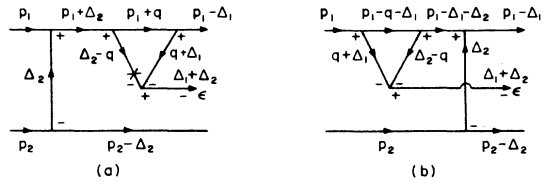

FIG. 18. (a) Feynman diagrams 5-8. (b) Feynman diagram 5-9.

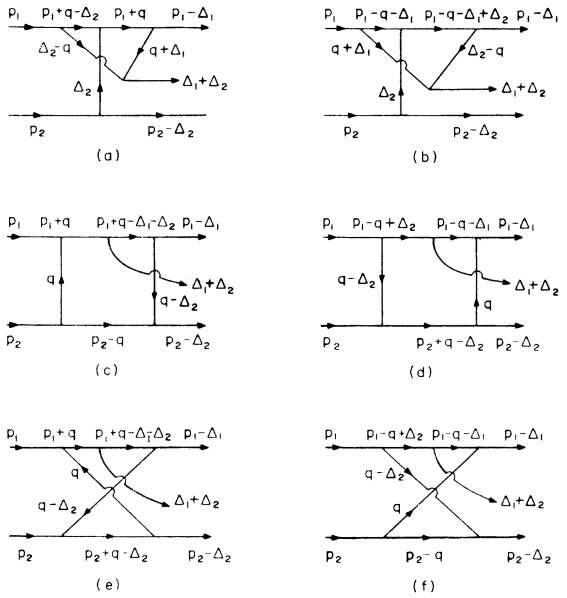

FIG. 19. Diagrammatic argument that Feynman diagrams 5-10 (a,b), 5-11 (c,d), and 5-12 (e,f) do not contribute to leading order.

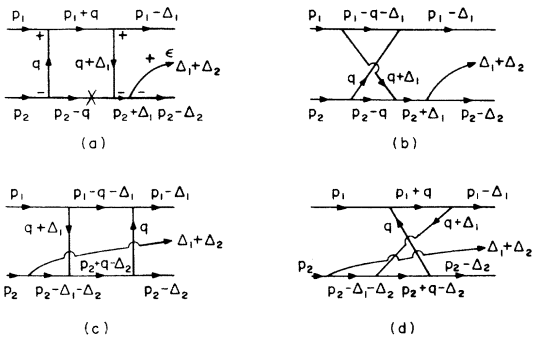

FIG. 20. Feynman diagrams (a) 5-13, (b) 5-14, (c) 5-15, and (d) 5-16.

The only nonzero contribution comes from the region (3.5), and then the contour is closed in the upper half-plane about the pole at (3.4c). Once again, the dominant contribution from the q_- integration comes from the region (3.7), and so

$$M_8^{(5)} \sim g^5 s \ln\left(\frac{s_1}{\lambda^2}\right) \frac{1}{\vec{\Delta}_{2\perp}^{\,2}+\lambda^2} \frac{\epsilon_-}{k_-} \int \frac{d^2\vec{q}_\perp}{(2\pi)^3} \frac{1}{\vec{q}_\perp^{\,2}+\lambda^2} \quad , \tag{3.26}$$

where the origin has been translated in the logarithmically divergent integral.

Feynman diagram 5-9 is shown in Fig. 18(b). By comparison with diagram 5-8 in Fig. 18(a),

$$M_9^{(5)} \sim -M_8^{(5)} \quad . \tag{3.27}$$

From the isospin identity of Fig. 12, $I_8^{(5)} = I_2^{(3)}$ and $I_9^{(5)} = I_3^{(3)}$, so from (2.15),

$$\mathfrak{M}_8^{(5)} + \mathfrak{M}_9^{(5)} \sim M_8^{(5)} I_1^{(3)} \quad . \tag{3.28}$$

Figure 19 shows Feynman diagrams 5-10, 5-11, and 5-12, each drawn with two different internal momentum flows; comparison of the propagators and internal vertices of these pairs shows that none of them contributes to leading order.

Feynman diagrams 5-13 through 5-16 are drawn in Fig. 20:

$$M_{13}^{(5)} \sim \tfrac{1}{2}(-i)^{11} g^5 \left(\frac{2p_{1+}}{\sqrt{2}}\right)^2 \left(\frac{-2p_{2-}}{\sqrt{2}}\right)^3 \frac{1}{p_{2-}k_+} \frac{\epsilon_+}{\sqrt{2}} \int \frac{d^2\vec{q}_\perp}{(2\pi)^4} \int dq_- \int dq_+ \frac{1}{D_{13}} \quad , \tag{3.29}$$

where

$$D_{13} \sim [(p_{2-}-q_-)(p_{2+}-q_+) - \vec{q}_\perp^{\,2} - \lambda^2 + i\epsilon]\,(q_+q_- - \vec{q}_\perp^{\,2} - \lambda^2 + i\epsilon)[(p_{1+}+q_+)q_- - \vec{q}_\perp^{\,2} - \lambda^2 + i\epsilon]$$
$$\times [(q_+ + \Delta_{1+})q_- - (\vec{q}_\perp + \vec{\Delta}_{1\perp})^2 - \lambda^2 + i\epsilon] \quad . \tag{3.30}$$

The integration is negligible unless

$$\frac{\lambda^2}{p_{1+}} \ll q_- \ll p_{2-} \quad , \tag{3.31}$$

in which case the contour is closed in the upper half-plane about the pole at

$$q_+ = p_{2+} - \frac{\vec{q}_\perp^{\,2} + \lambda^2 - i\epsilon}{p_{2-} - q_-} = O\left(\frac{1}{p_{2-}}\right) \quad . \tag{3.32}$$

Then the q_- integral is approximately

$$\int_{\lambda^2/p_{1+}}^{p_{2-}} dq_- \frac{1}{q_-(q_-k_+ - (\vec{q}_\perp + \vec{\Delta}_{1\perp})^2 - \lambda^2 + i\epsilon)} = \frac{-1}{(\vec{q}_\perp + \vec{\Delta}_{1\perp})^2 + \lambda^2} \ln\left[\frac{q_-}{q_-k_+ - (\vec{q}_\perp + \vec{\Delta}_{1\perp})^2 - \lambda^2 + i\epsilon}\right]_{\lambda^2/p_{1+}}^{p_{2-}}$$
$$\sim \frac{-1}{(\vec{q}_\perp + \vec{\Delta}_{1\perp})^2 + \lambda^2} \ln\left(\frac{s_1}{\lambda^2}\right) \quad . \tag{3.33}$$

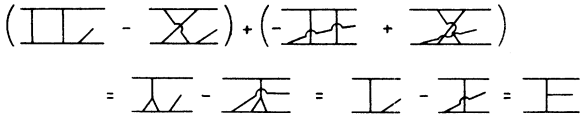

FIG. 21. Diagrammatic calculation of the isospin associated with the combined amplitudes of Feynman diagrams 5-13 through 5-16.

Thus, in effect, the $q_-k_+ - (\vec{q}_\perp + \vec{\Delta}_{1\perp})^2 - \lambda^2$ term in the denominator acts as a cutoff; there is no contribution to the leading order unless $q_-k_+ \ll 1$, in which case the integral becomes

$$\frac{-1}{(\vec{q}_\perp + \Delta_{1\perp})^2 + \lambda^2} \int_{\lambda^2/p_{1+}}^{k_-} \frac{dq_-}{q_-} \quad , \tag{3.34}$$

which gives the same answer as before. It follows that

$$M_{13}^{(5)} \sim -2g^5 s \ln\left(\frac{s_1}{\lambda^2}\right) \frac{\epsilon_+}{k_+} \times \int \frac{d^2\vec{q}_\perp}{(2\pi)^3} \frac{1}{(\vec{q}_\perp^{\,2} + \lambda^2)[(\vec{q}_\perp + \vec{\Delta}_{1\perp})^2 + \lambda^2]} \quad . \tag{3.35}$$

From Fig. 20, by comparing propagators on the high-momentum lines,

$$-M_{14}^{(5)} \sim -M_{15}^{(5)} \sim M_{16}^{(5)} \sim M_{13}^{(5)} \quad . \tag{3.36}$$

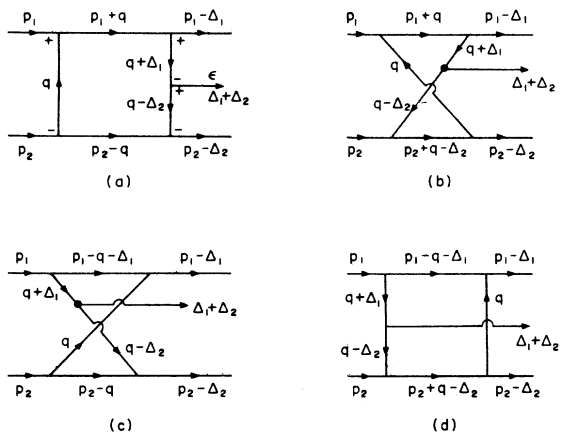

FIG. 22. Feynman diagrams (a) 5-33, (b) 5-34, (c) 5-35, and (d) 5-36.

A diagrammatic calculation of the isospin, using the identities of Figs. 8 and 12, is given in Fig. 21 and shows that

$$I_{13}^{(5)} - I_{14}^{(5)} - I_{15}^{(5)} + I_{16}^{(5)} = I_1^{(3)} \quad , \tag{3.37}$$

so that

$$\mathfrak{M}_{13}^{(5)} + \mathfrak{M}_{14}^{(5)} + \mathfrak{M}_{15}^{(5)} + \mathfrak{M}_{16}^{(5)} \sim M_{13}^{(5)} I_1^{(3)} \quad . \tag{3.38}$$

Therefore, from (3.11), (3.13), (3.14), (3.15), (3.21), (3.23), (3.26), (3.28), (3.35), and (3.38),

$$\sum_{i=1}^{16} \mathfrak{M}_i^{(5)} \sim g^5 s \ln\left(\frac{s_1}{\lambda^2}\right) \frac{1}{\vec{\Delta}_{2\perp}^{\,2} + \lambda^2} \int \frac{d^2\vec{q}_\perp}{(2\pi)^3} \frac{1}{(\vec{q}_\perp^{\,2} + \lambda^2)[(\vec{q}_\perp + \vec{\Delta}_{1\perp})^2 + \lambda^2]} \times \left[\vec{\epsilon}_\perp \cdot (3\vec{\Delta}_{2\perp} - \vec{\Delta}_{1\perp}) + \epsilon_+ k_- \left(\frac{1}{2} - 2\,\frac{\vec{\Delta}_{2\perp}^{\,2} + \lambda^2}{\vec{k}_\perp^{\,2} + \lambda^2}\right) + \frac{\epsilon_-}{k_-}\left(-\tfrac{3}{2}(\vec{k}_\perp^{\,2} + \lambda^2) + 2(\vec{\Delta}_{1\perp}^{\,2} + \lambda^2) - (\vec{\Delta}_{2\perp}^{\,2} + \lambda^2)\right)\right] \quad . \tag{3.39}$$

Note that the transverse momentum integration in (3.39) is convergent.

Feynman diagrams 5-17 through 5-32 are obtained by reflecting diagrams 5-1 through 5-16 respectively through a horizontal plane mirror, which is equivalent to the transformation (2.11) with a minus sign added. Thus

$$\sum_{i=17}^{32} \mathfrak{M}_i^{(5)} \sim -g^5 s \ln\left(\frac{s_2}{\lambda^2}\right) \frac{1}{\vec{\Delta}_{1\perp}^{\,2} + \lambda^2} \int \frac{d^2\vec{q}_\perp}{(2\pi)^3} \frac{1}{(\vec{q}_\perp^{\,2} + \lambda^2)[(\vec{q}_\perp + \vec{\Delta}_{2\perp})^2 + \lambda^2]} \times \left[\vec{\epsilon}_\perp \cdot (3\vec{\Delta}_{1\perp} - \vec{\Delta}_{2\perp}) + \epsilon_- k_+ \left(\frac{1}{2} - 2\,\frac{\vec{\Delta}_{1\perp}^{\,2} + \lambda^2}{\vec{k}_\perp^{\,2} + \lambda^2}\right) + \frac{\epsilon_+}{k_+}\left(-\tfrac{3}{2}(\vec{k}_\perp^{\,2} + \lambda^2) + 2(\vec{\Delta}_{2\perp}^{\,2} + \lambda^2) - (\vec{\Delta}_{1\perp}^{\,2} + \lambda^2)\right)\right] . \tag{3.40}$$

Feynman diagram 5-33 is shown in Fig. 22(a). Its space-time amplitude is

$$M_{33}^{(5)} \sim \tfrac{1}{2}(-i)^{11} g^5 \left(\frac{2p_{1+}}{\sqrt{2}}\right)^2 \left(\frac{-2p_{2-}}{\sqrt{2}}\right)^2 \int \frac{d^2\vec{q}_\perp}{(2\pi)^4} \int dq_- \int dq_+ \frac{\Gamma}{D_{33}} \quad , \tag{3.41}$$

where

$$\Gamma \sim -\vec{\epsilon}_\perp \cdot (\vec{\Delta}_{2\perp} - \vec{\Delta}_{1\perp} - 2\vec{q}_\perp) - \tfrac{1}{2}\epsilon_+(k_- + q_-) + \tfrac{1}{2}\epsilon_-(k_+ - q_+) \tag{3.42}$$

and

$$D_{33}\sim p_{1+}q_{-}[(p_{2-}-q_{-})(p_{2+}-q_{+})-\vec{q}_{\perp}^{\,2}-\lambda^2+i\epsilon]\,(q_{+}q_{-}-\vec{q}_{\perp}^{\,2}-\lambda^2+i\epsilon)$$
$$\times[(q_{+}+k_{+})q_{-}-(\vec{q}_{\perp}+\vec{\Delta}_{1\perp})^2-\lambda^2+i\epsilon][(q_{-}-\Delta_{2-})q_{+}-(\vec{q}_{\perp}-\vec{\Delta}_{2\perp})^2-\lambda^2+i\epsilon]\ . \tag{3.43}$$

There are two regions where the q_+ integration is nonzero: region A, where

$$\Delta_{2-}<q_{-}<p_{2-} \tag{3.44}$$

and region B, where

$$0<q_{-}<\Delta_{2-}\ . \tag{3.45}$$

In region A, the contour is closed in the upper half-plane about the pole given in (3.32). In order for the q_- integration to give a contribution proportional to $\ln(s_2/\lambda^2)$, Γ in (3.42) must be proportional to q_-; then the dominant contribution comes from

$$k_{-}\ll q_{-}\ll p_{2-} \tag{3.46}$$

and

$$\int dq_{-}\int dq_{+}\,\frac{\Gamma}{D_{33}}\sim -2\pi i\int_{k_{-}}^{p_{2-}}dq_{-}\,\frac{-\frac{1}{2}\epsilon_{+}q_{-}}{p_{1+}p_{2-}k_{+}q_{-}{}^2(\vec{q}_{\perp}^{\,2}+\lambda^2)[(\vec{q}_{\perp}-\vec{\Delta}_{2\perp})^2+\lambda^2]}$$
$$\sim\frac{\pi i}{p_{1+}p_{2-}}\,\frac{\epsilon_{+}}{k_{+}}\ln\left(\frac{s_2}{\lambda^2}\right)\frac{1}{(\vec{q}_{\perp}^{\,2}+\lambda^2)[(\vec{q}_{\perp}-\vec{\Delta}_{2\perp})^2+\lambda^2]}\ . \tag{3.47}$$

Thus the contribution to $M_{33}^{(5)}$ from region A is

$$-g^5 s\ln\left(\frac{s_2}{\lambda^2}\right)\frac{\epsilon_{+}}{k_{+}}\int\frac{d^2\vec{q}_{\perp}}{(2\pi)^3}\,\frac{1}{(\vec{q}_{\perp}^{\,2}+\lambda^2)[(\vec{q}_{\perp}-\vec{\Delta}_{2\perp})^2+\lambda^2]}\ . \tag{3.48}$$

In region B, the contour is again closed in the upper half-plane, but now there are two poles, that of (3.32) and

$$q_{+}=-\frac{(\vec{\Delta}_{2\perp}-\vec{q}_{\perp})^2+\lambda^2-i\epsilon}{\Delta_{2-}-q_{-}}\ . \tag{3.49}$$

For the pole given in (3.32),

$$\int dq_{+}\,\frac{\Gamma}{D_{33}}\sim\frac{2\pi i}{p_{1+}p_{2-}}\,\frac{\Gamma}{q_{-}(\vec{q}_{\perp}^{\,2}+\lambda^2)[(\vec{q}_{\perp}+\vec{\Delta}_{1\perp})^2+\lambda^2][(\vec{q}_{\perp}-\vec{\Delta}_{2\perp})^2+\lambda^2]} \tag{3.50}$$

since the dominant contribution comes from the interval given in (3.7). For the pole given in (3.49), again using (3.7),

$$\int dq_{+}\,\frac{\Gamma}{D_{33}}\sim\frac{-2\pi i}{k_{-}}\,\frac{\Gamma}{p_{1+}q_{-}p_{2-}\{[(\vec{\Delta}_{2\perp}-\vec{q}_{\perp})^2+\lambda^2]/k_{-}\}(\vec{q}_{\perp}^{\,2}+\lambda^2)[(\vec{q}_{\perp}+\vec{\Delta}_{1\perp})^2+\lambda^2]} \tag{3.51}$$

Therefore, (3.50) and (3.51) cancel except for the term in Γ proportional to q_+. For the pole of (3.32) this contribution is too small, but for the pole given by (3.49),

$$\Gamma\sim\frac{1}{2}\,\frac{\epsilon_{-}}{k_{-}}[(\vec{\Delta}_{2\perp}-\vec{q}_{\perp})^2+\lambda^2] \tag{3.52}$$

so that the contribution to $M_{33}^{(5)}$ from region B is

$$g^5 s\ln\left(\frac{s_1}{\lambda^2}\right)\frac{\epsilon_{-}}{k_{-}}\int\frac{d^2\vec{q}_{\perp}}{(2\pi)^3}\,\frac{1}{(\vec{q}_{\perp}^{\,2}+\lambda^2)[(\vec{q}_{\perp}+\vec{\Delta}_{1\perp})^2+\lambda^2]}\ . \tag{3.53}$$

Adding (3.48) and (3.53) gives

$$M_{33}^{(5)}\sim g^5 s\ln\left(\frac{s_1}{\lambda^2}\right)\frac{\epsilon_{-}}{k_{-}}\int\frac{d^2\vec{q}_{\perp}}{(2\pi)^3}\,\frac{1}{(\vec{q}_{\perp}^{\,2}+\lambda^2)[(\vec{q}_{\perp}+\vec{\Delta}_{1\perp})^2+\lambda^2]}-g^5 s\ln\left(\frac{s_2}{\lambda^2}\right)\frac{\epsilon_{+}}{k_{+}}\int\frac{d^2\vec{q}_{\perp}}{(2\pi)^3}\,\frac{1}{(\vec{q}_{\perp}^{\,2}+\lambda^2)[(\vec{q}_{\perp}+\vec{\Delta}_{2\perp})^2+\lambda^2]}\ . \tag{3.54}$$

A comparison of the propagators on the large momentum lines in the diagrams of Fig. 22 shows that

$$-M_{34}^{(5)}\sim -M_{35}^{(5)}\sim M_{36}^{(5)}\sim M_{33}^{(5)}\ . \tag{3.55}$$

A calculation of the diagrams' isospin, carried out diagrammatically in Fig. 23, shows that

$$I_{33}^{(5)} - I_{34}^{(5)} - I_{35}^{(5)} + I_{36}^{(5)} = I_1^{(3)} \tag{3.56}$$

so that

$$\mathfrak{M}_{33}^{(5)} + \mathfrak{M}_{34}^{(5)} + \mathfrak{M}_{35}^{(5)} + \mathfrak{M}_{36}^{(5)} \sim M_{33}^{(5)} I_3^{(1)} . \tag{3.57}$$

Adding together the contributions from all the diagrams, using (3.39), (3.40), (3.54), and (3.57),

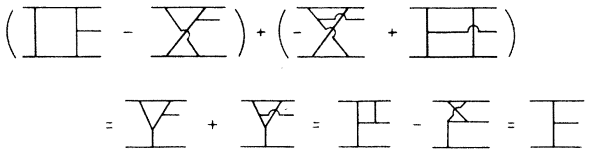

FIG. 23. Diagrammatic calculation of the isospin associated with the combined amplitudes of Feynman diagrams 5-33 through 5-36.

$$M^{(5)} = \sum_{i=1}^{36} M_i^{(5)} \sim g^5 s \ln\left(\frac{s_1}{\lambda^2}\right) \frac{1}{\vec{\Delta}_{2\perp}^{\,2}+\lambda^2} \int \frac{d^2\vec{q}_\perp}{(2\pi)^3} \frac{1}{(\vec{q}_\perp^{\,2}+\lambda^2)[(\vec{q}_\perp+\vec{\Delta}_{1\perp})^2+\lambda^2]}$$
$$\times \left[\vec{\epsilon}_\perp \cdot (3\vec{\Delta}_{2\perp} - \vec{\Delta}_{1\perp}) + \epsilon_+ k_- \left(\tfrac{1}{2} - 2\,\frac{\vec{\Delta}_{2\perp}^{\,2}+\lambda^2}{\vec{k}_\perp^{\,2}+\lambda^2}\right) + \epsilon_- k_+ \left(-\tfrac{3}{2} + 2\,\frac{\vec{\Delta}_{1\perp}^{\,2}+\lambda^2}{\vec{k}_\perp^{\,2}+\lambda^2}\right)\right] - (1 \leftrightarrow 2, + \leftrightarrow -) . \tag{3.58}$$

By gauge invariance

$$0 = \epsilon \cdot k = \tfrac{1}{2}\epsilon_+ k_- + \tfrac{1}{2}\epsilon_- k_+ - \vec{\epsilon}_\perp \cdot (\vec{\Delta}_{1\perp} + \vec{\Delta}_{2\perp}) , \tag{3.59}$$

so adding zero to (3.58) in the form

$$g^5 s \ln\left(\frac{s_1}{\lambda^2}\right) \frac{1}{\vec{\Delta}_{2\perp}^{\,2}+\lambda^2} \int \frac{d^2\vec{q}_\perp}{(2\pi)^3} \frac{1}{(\vec{q}_\perp^{\,2}+\lambda^2)[(\vec{q}_\perp+\vec{\Delta}_{1\perp})^2+\lambda^2]} (\epsilon \cdot k) - (1 \leftrightarrow 2, + \leftrightarrow -) \tag{3.60}$$

gives

$$\mathfrak{M}^{(5)} \sim g^3 \frac{2s}{(\vec{\Delta}_{1\perp}^{\,2}+\lambda^2)(\vec{\Delta}_{2\perp}^{\,2}+\lambda^2)} \left[\vec{\epsilon}_\perp \cdot (\vec{\Delta}_{1\perp} - \vec{\Delta}_{2\perp}) - \epsilon_+ k_- \left(\tfrac{1}{2} - \frac{\vec{\Delta}_{2\perp}^{\,2}+\lambda^2}{\vec{k}_\perp^{\,2}+\lambda^2}\right) + \epsilon_- k_+ \left(\tfrac{1}{2} - \frac{\vec{\Delta}_{1\perp}^{\,2}+\lambda^2}{\vec{k}_\perp^{\,2}+\lambda^2}\right)\right]$$
$$\times \left[-\alpha(\vec{\Delta}_{1\perp}) \ln\left(\frac{s_1}{\lambda^2}\right) - \alpha(\vec{\Delta}_{2\perp}) \ln\left(\frac{s_2}{\lambda^2}\right)\right] I_1^{(3)} , \tag{3.61}$$

where $\alpha(\vec{\Delta})$ was defined in (1.2). This result is identical with the fifth-order part of (1.1).

For scalar production in the fifth order, only four diagrams contribute; these are given in Fig. 24. A simple calculation shows that together they give the amplitude

$$M_S^{(5)} \sim +2\lambda g^3 s \frac{1}{(\vec{\Delta}_{1\perp}^{\,2}+\lambda^2)(\vec{\Delta}_{2\perp}^{\,2}+\lambda^2)} \left[\alpha(\vec{\Delta}_{1\perp}) \ln\left(\frac{s_1}{\lambda^2}\right) + \alpha(\vec{\Delta}_{2\perp}) \ln\left(\frac{s_2}{\lambda^2}\right)\right] \tag{3.62}$$

with the isospin that of the diagram in Fig. 2(b). This also agrees with (1.1) in the fifth order.

IV. THE SEVENTH-ORDER DIAGRAMS

Since the seventh-order calculation is very similar to that of arbitrary orders, it will not be done separately. However, it is important to know which diagrams contribute, at least to the convergent part of the amplitude,[14] so that one may infer which diagrams contribute in higher orders. All such diagrams are given in Fig. 25. In this, and in all higher orders, it is assumed that the transverse-momentum integrals converge, so divergent parts are discarded.

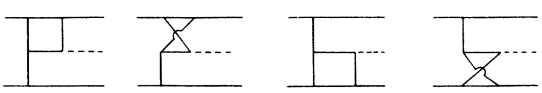

FIG. 24. The four fifth-order Feynman diagrams which contribute to scalar production.

V. ARBITRARY ORDERS

Diagrams which give convergent contributions to arbitrary orders are of the form of those of seventh and lower orders, with extra horizontal lines added to make more closed loops. The general types are shown in Fig. 26; all diagrams formed by twisting the top or bottom horizontal lines, by reflecting through a horizontal plane mirror, or by a combination of these processes also contribute.

In order to streamline the calculation, all q_+ integrations will be implicit. They will be done by contour integration, with momentum-flow dia-

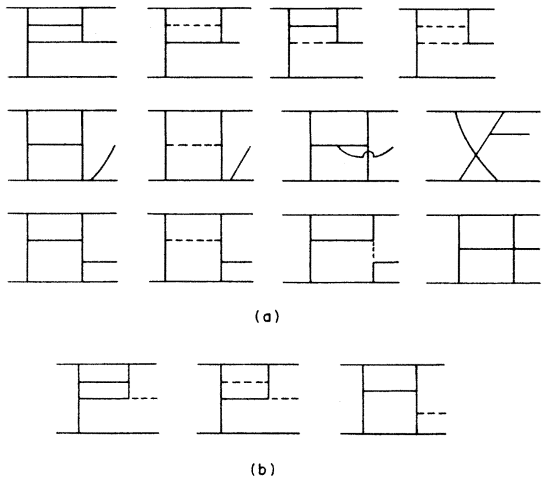

FIG. 25. Feynman diagrams which contribute to the convergent part of the seventh-order amplitude for (a) vector-meson production and (b) scalar production. All diagrams formed by twisting the upper or lower horizontal lines or by reflection through a horizontal plane mirror also contribute.

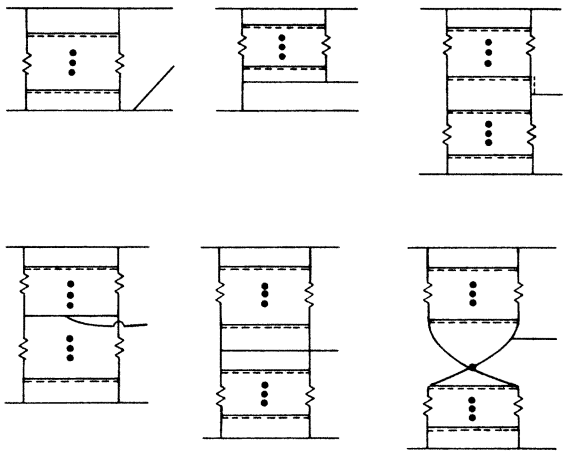

FIG. 26. The general types of diagrams which contribute to the convergent part of the amplitude to arbitrary orders. All diagrams formed by twisting the top or bottom horizontal lines, by reflecting through a horizontal plane mirror, or by a combination of these processes also contribute. Solid and dashed double lines stand for either a vector (solid) or scalar (dashed) particle.

grams[15] used to indicate which poles in the complex q_+ plane are enclosed by the contour. Momentum-flow diagrams are similar to Feynman diagrams, except that the arrow associated with the momentum of each line has a special meaning. For a line carrying four-momentum q, the arrow points in the direction of positive q_-. There may be several momentum-flow diagrams corresponding to each Feynman diagram. For any closed loop, if all the arrows point in the same direction of flow, whether clockwise or counterclockwise, the q_+ integration is zero. If arrows of a given loop point in both directions, then specify one direction; contributions from all the poles corresponding to lines with arrows pointing in that direction must be added together. The two choices of direction correspond to closing the contour in the upper or the lower half of the q_+ plane. If there is only one pole, the line corresponding to it in the flow diagram will be marked by a cross (×). If there are two or more poles, the corresponding lines will be marked by double slashes(//). Each integration over a pole of the form $1/(Aq_+ + B + i\epsilon)$ introduces a factor of $-2\pi i/|A|$.

Momentum-flow diagram Ia is shown in Fig. 27 (a). It is the only possible (nonzero) flow diagram associated with the corresponding Feynman diagram. It has n closed loops and $2n+3$ vertices.

The space-time amplitude is

$$M_I^a \sim (-i)^{1+(2n+3)+(3n+2)} g^{2n+3} \left(\frac{2p_{1+}}{\sqrt{2}}\right)^2 \left(\frac{-2p_{2-}}{\sqrt{2}}\right)^3 \frac{1}{p_{2-}k_+} \frac{\epsilon_+}{\sqrt{2}} \left(\frac{-i}{2}\right)^n \prod_{i=1}^{n} \int \frac{d^2\vec{q}_{i\perp}}{(2\pi)^3} \prod_{j=1}^{n} \int dq_{j-} \frac{N}{D}. \quad (5.1)$$

Here N represents the vertex factors and will be determined below,

$$D \sim p_{1+}p_{2-}q_{n-} \prod_{i=1}^{n-1} (q_{i-} - q_{i+1-}) \prod_{j=1}^{n} (q_{j+}q_{j-} - a_j + i\epsilon) \prod_{l=1}^{n} ((q_{l+} + k_+)q_{l-} - b_l + i\epsilon), \quad (5.2)$$

$$q_{1+} = p_{2+} - \frac{(\vec{p}_{2\perp} - \vec{q}_{1\perp})^2 + \lambda^2}{p_{2-} - q_{1-}} \quad (5.3a)$$

and

$$q_{i+} - q_{i+1+} = \frac{c_i}{q_{i-} - q_{i+1-}}, \quad i = 1, \ldots, n-1, \quad (5.3b)$$

where

$$a_i = \vec{q}_{i\perp}^{\,2} + \lambda^2, \quad i = 1, \ldots, n \quad (5.4a)$$

$$b_i = (\vec{q}_{i\perp} + \vec{\Delta}_{1\perp})^2 + \lambda^2, \quad i = 1, \ldots, n \quad (5.4b)$$

and

$$c_i = (\vec{q}_{i\perp} - \vec{q}_{i+1\perp})^2 + \lambda^2, \quad i = 1, \ldots, n-1. \tag{5.4c}$$

The region of integration is read directly off of the flow diagram since each arrow points in the direction of positive momentum:

$$0 < q_{n-} < q_{n-1-} < \cdots < q_{1-} < p_{2-}. \tag{5.5}$$

The region which gives the dominant contribution is

$$\frac{\lambda^2}{p_{1+}} \ll q_{n-} \ll q_{n-1-} \ll \cdots \ll q_{1-} \ll p_{2-}, \tag{5.6}$$

so that

$$q_{1+} = O\left(\frac{1}{p_{2-}}\right), \tag{5.7a}$$

$$q_{i+} \sim -\frac{c_{i-1}}{q_{i-1-}}, \quad i = 2, \ldots, n, \tag{5.7b}$$

and

$$D \sim p_{1+} p_{2-} \left(\prod_{i=1}^{n} q_{i-}\right) \prod_{j=1}^{n} (-a_j) \prod_{i=1}^{n} (k_+ q_{i-} - b_i). \tag{5.8}$$

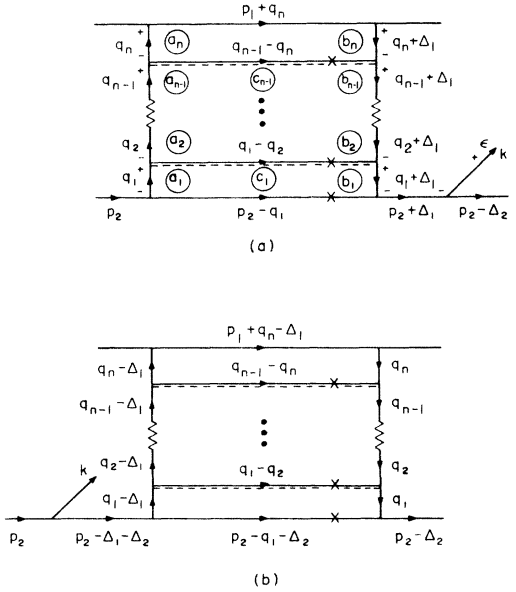

FIG. 27. Momentum-flow diagrams Ia and Ib. The circled letter next to a line with momentum q stands for $\vec{q}_\perp^{\,2} + \lambda^2$.

Suppose that $q_{i+1} \ll k_- \ll q_{i-}$ for some i. The integration over the $-$ momenta is then proportional to

$$\frac{1}{\prod_{j=1}^{n}(-a_j)} \int_{k-}^{p_{2-}} \frac{dq_{1-}}{q_{1-}(k_+ q_{1-} - b_1)} \cdots \int_{k-}^{q_{i-1-}} \frac{dq_{i-}}{q_{i-}(k_+ q_{i-} - b_i)} \int_{\lambda^2/p_{1+}}^{k-} \frac{dq_{i+1-}}{q_{i+1-}(-b_{i+1})} \cdots \int_{\lambda^2/p_{1+}}^{q_{n-1-}} \frac{dq_{n-}}{q_{n-}(-b_n)} N. \tag{5.9}$$

This is divergent in the transverse-momentum integration if N is proportional to any of q_{1-} through q_{i-}, and is too small otherwise (i.e., it produces less than n logarithms). So the only convergent contribution comes when $k_- \gg q_{1-}$. The $-$ momentum integration is then like

$$\frac{1}{\left(\prod_{i=1}^{n} a_i\right)\left(\prod_{j=1}^{n} b_j\right)} \int_{\lambda^2/p_{1+}}^{k-} \frac{dq_{1-}}{q_{1-}} \cdots \int_{\lambda^2/p_{1+}}^{q_{n-1-}} \frac{dq_{n-}}{q_{n-}} N. \tag{5.10}$$

It is now crucial to determine which polarizations of the internal lines give the largest contributions. Since $q_{i+} \gg q_{j+}$ and $q_{i-} \ll q_{j-}$ if $i > j$, it seems reasonable that along each vertical line of Fig. 27 (i.e., those with momenta q_i or $q_i \pm \Delta_1$) the polarization should be $+$ at the top and $-$ at the bottom, as indicated in Fig. 27(a). This is in fact correct. A proof is given in the Appendix.

In order to calculate N, consider a typical horizontal line or "rung" as shown in Fig. 28(a). With notation given in the figure, the product of the two vertex factors is

$$\begin{aligned} q_{i-}q_{i+1+} &- (\vec{q}_{i\perp} + \vec{q}_{i+1\perp}) \cdot (\vec{q}_{i\perp} + \vec{q}_{i+1\perp} + 2\vec{\Delta}_{1\perp}) \\ &\sim -a_i - a_{i+1} - b_i - b_{i+1} + 2(\vec{\Delta}_{1\perp}^{\,2} + \lambda^2) + \lambda^2 \\ &\Rightarrow 2(\vec{\Delta}_{1\perp}^{\,2} + \lambda^2) + \lambda^2, \end{aligned}$$

where the three possible internal polarizations have been summed over and where the arrow ($\Rightarrow$) indicates that divergent terms have been dropped.

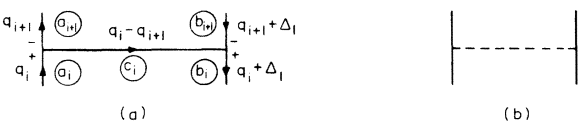

FIG. 28. A section from a typical diagram. The horizontal line is either a vector meson (a) or a scalar (b).

If a scalar particle replaces the vector meson, as in Fig. 28(b), (5.11) is replaced by $-(-\lambda)^2$, where the minus sign comes from the sign difference between the vector and scalar propagators. It will be shown below that the overall isospin factor is independent of whether the horizontal line is a vector or scalar, so that their space-time amplitudes may be added together to give $2(\vec{\Delta}_{1\perp}^2+\lambda^2)$. Since there are $n-1$ such rungs,

$$N\sim[2(\vec{\Delta}_{1\perp}^2+\lambda^2)]^{n-1}. \tag{5.12}$$

Because

$$\int_{\lambda^2/p_{1+}}^{k_-}\frac{dq_{1-}}{q_{1-}}\cdots\int_{\lambda^2/p_{1+}}^{q_{n-1-}}\frac{dq_{n-}}{q_{n-}}\sim\frac{\ln^n(s_1/\lambda^2)}{n!}, \tag{5.13}$$

$$M_{\rm I}^a\sim(-1)^n 2g^{2n+3}s\,\frac{\ln^n(s_1/\lambda^2)}{n!}\,\frac{\epsilon_+}{k_+}\,(\vec{\Delta}_{1\perp}^2+\lambda^2)^{n-1}K_1^n, \tag{5.14}$$

where

$$K_1=K(\vec{\Delta}_{1\perp})=\int\frac{d^2\vec{q}_\perp}{(2\pi)^3}\,\frac{1}{\vec{q}_\perp^2+\lambda^2}\,\frac{1}{(\vec{q}_\perp+\vec{\Delta}_{1\perp})^2+\lambda^2}. \tag{5.15}$$

A similar analysis of momentum-flow diagram Ib shows that

$$M_{\rm I}^b\sim -M_{\rm I}^a. \tag{5.16}$$

This can also be seen by comparing propagators and vertices on the corresponding Feynman diagrams. Let the diagrams formed from diagram Ia (Ib) by twisting the top horizontal line be called Ic (Id). Clearly,

$$-M_{\rm I}^c\sim M_{\rm I}^d\sim M_{\rm I}^a. \tag{5.17}$$

The isospin calculation carried out in Fig. 29(a) shows that

$$I_{\rm I}^a-I_{\rm I}^b-I_{\rm I}^c+I_{\rm I}^d=I_1^{(3)} \tag{5.18}$$

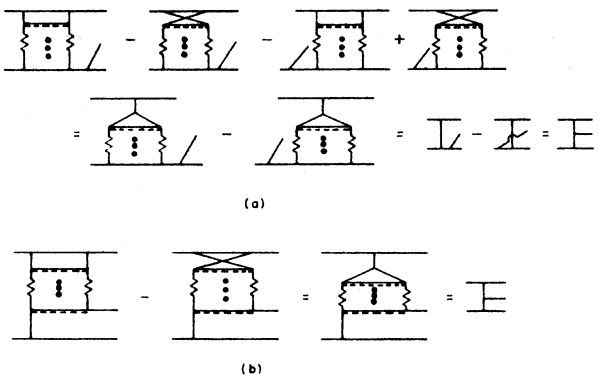

FIG. 29. The isospin calculation for diagrams (a) I and (b) II.

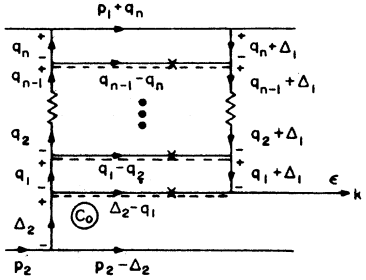

FIG. 30. Momentum-flow diagram IIa.

whether the horizontal lines are vector or scalar particles, and so

$$\mathfrak{M}_{\rm I}=\mathfrak{M}_{\rm I}^a+\mathfrak{M}_{\rm I}^b+\mathfrak{M}_{\rm I}^c+\mathfrak{M}_{\rm I}^d\sim M_{\rm I}^a I_1^{(3)}. \tag{5.19}$$

Momentum-flow diagram IIa is shown in Fig. 30. It is the only flow diagram associated with the corresponding Feynman diagram. Its space-time amplitude is

$$M_{\rm II}^a\sim(-i)^{5n+6}g^{2n+3}\left(\frac{2p_{1+}}{\sqrt{2}}\right)^2\left(\frac{-2p_{2-}}{\sqrt{2}}\right)\frac{-1}{\vec{\Delta}_{2\perp}^2+\lambda^2}\times\left(\frac{-i}{2}\right)^n\prod_{i=1}^{n}\int\frac{d^2\vec{q}_{i\perp}}{(2\pi)^3}\prod_{j=1}^{n}\int dq_{j-}\,\frac{N}{D}. \tag{5.20}$$

Since the region which gives the dominant contribution is

$$\frac{\lambda^2}{p_{1+}}\ll q_{n-}\ll\cdots\ll q_{1-}\ll k_-, \tag{5.21}$$

and since

$$q_{1+}\sim\frac{-c_0}{k_-}, \tag{5.22a}$$

and

$$q_{i+}\sim\frac{-c_{i-1}}{q_{i-1-}},\quad i=2,\ldots,n \tag{5.22b}$$

$$D\sim p_{1+}k_-\left(\prod_{i=1}^{n}q_{i-}\right)\left(\prod_{j=1}^{n}a_j\right)\left(\prod_{k=1}^{n}b_k\right), \tag{5.23}$$

where

$$c_0=(\vec{\Delta}_{2\perp}-\vec{q}_{1\perp})^2+\lambda^2, \tag{5.24}$$

and a_i, b_i, c_i are given by (5.4). Again the polarization of all the vertical lines is + at the top, − at the bottom (see the Appendix). Therefore, summing over all polarizations of the horizontal lines,

$$N\sim\frac{k_-}{\sqrt{2}}[2(\vec{\Delta}_{1\perp}^2+\lambda^2)]^{n-1}\times\Big\{\vec{\epsilon}_\perp\cdot(3\vec{\Delta}_{2\perp}-\vec{\Delta}_{1\perp})+\tfrac{1}{2}\epsilon_+k_-+\frac{\epsilon_-}{k_-}[-\tfrac{3}{2}(\vec{k}_\perp^2+\lambda^2)+2(\vec{\Delta}_{1\perp}^2+\lambda^2)-(\vec{\Delta}_{2\perp}^2+\lambda^2)]\Big\}, \tag{5.25}$$

where the divergent terms have been dropped and where the contributions from the scalar and vector horizontal lines have been added together, since their isospin factors are effectively equal (see below). Then

$$M_{\mathrm{II}}^{a} \sim (-1)^{n+1} g^{2n+3} s \frac{\ln^n(s_1/\lambda^2)}{n!} \frac{1}{\vec{\Delta}_{2\perp}^{\,2}+\lambda^2} (\vec{\Delta}_{1\perp}^{\,2}+\lambda^2)^{n-1} K_1^{\,n}$$
$$\times \left[\vec{\epsilon}_\perp \cdot (3\vec{\Delta}_{2\perp} - \vec{\Delta}_{1\perp}) + \tfrac{1}{2}\epsilon_+ k_- + \frac{\epsilon_-}{k_-} (-\tfrac{3}{2}(\vec{k}_\perp^{\,2}+\lambda^2) + 2(\vec{\Delta}_{1\perp}^{\,2}+\lambda^2) - (\vec{\Delta}_{2\perp}^{\,2}+\lambda^2)) \right]. \tag{5.26}$$

Since $\epsilon \cdot k = 0$ by gauge invariance,

$$(-1)^{n+1} g^{2n+3} s \frac{\ln^n(s_1/\lambda^2)}{n!} \frac{(\vec{\Delta}_{1\perp}^{\,2}+\lambda^2)^{n-1}}{\vec{\Delta}_{2\perp}^{\,2}+\lambda^2} K_1^{\,n} (\epsilon \cdot k)$$

can be added to (5.26) to give

$$M_{\mathrm{II}}^{a} \sim (-1)^n 2 g^{2n+3} s \frac{\ln^n(s_1/\lambda^2)}{n!} \frac{(\vec{\Delta}_{1\perp}^{\,2}+\lambda^2)^{n-1}}{\vec{\Delta}_{2\perp}^{\,2}+\lambda^2} K_1^{\,n} \left[\vec{\epsilon}_\perp \cdot (\vec{\Delta}_{1\perp} - \vec{\Delta}_{2\perp}) - \tfrac{1}{2}\epsilon_+ k_- \right.$$
$$\left. + \frac{1}{2} \frac{\epsilon_-}{k_-} (\vec{k}_\perp^{\,2}+\lambda^2 - 2(\vec{\Delta}_{1\perp}^{\,2}+\lambda^2) + \vec{\Delta}_{2\perp}^{\,2}+\lambda^2) \right]. \tag{5.27}$$

Diagram IIb is formed by twisting the top horizontal line of diagram IIa, so that $M_{\mathrm{II}}^{b} \sim -M_{\mathrm{II}}^{a}$. From Fig. 29(b), $I_{\mathrm{II}}^{a} - I_{\mathrm{II}}^{b} = I_1^{(3)}$ whether the horizontal lines are vectors or scalars, so that

$$\mathfrak{M}_{\mathrm{II}} = \mathfrak{M}_{\mathrm{II}}^{a} + \mathfrak{M}_{\mathrm{II}}^{b} \sim M_{\mathrm{II}}^{a} I_1^{(3)} . \tag{5.28}$$

The sets of diagrams formed by reflecting diagrams I and II through a horizontal plane mirror have the respective amplitudes [see (2.11)]

$$\bar{\mathfrak{M}}_{\mathrm{I}} \sim (-1)^{n+1} 2 g^{2n+3} s \frac{\ln^n(s_2/\lambda^2)}{n!} \frac{\epsilon_-}{k_-} (\vec{\Delta}_{2\perp}^{\,2}+\lambda^2)^{n-1} K_2^{\,n} I_1^{(3)} \tag{5.29}$$

and

$$\bar{\mathfrak{M}}_{\mathrm{II}} \sim (-1)^n 2 g^{2n+3} s \frac{\ln^n(s_2/\lambda^2)}{n!} \frac{(\vec{\Delta}_{2\perp}^{\,2}+\lambda^2)^{n-1}}{\vec{\Delta}_{1\perp}^{\,2}+\lambda^2} K_2^{\,n} I_1^{(3)}$$
$$\times \left[\vec{\epsilon}_\perp \cdot (\vec{\Delta}_{1\perp} - \vec{\Delta}_{2\perp}) + \tfrac{1}{2}\epsilon_- k_+ - \frac{1}{2} \frac{\epsilon_+}{k_+} (\vec{k}_\perp^{\,2}+\lambda^2 - 2(\vec{\Delta}_{2\perp}^{\,2}+\lambda^2) + \vec{\Delta}_{1\perp}^{\,2}+\lambda^2) \right], \tag{5.30}$$

where $K_2 = K(\vec{\Delta}_{2\perp})$ [see (5.15)].

Momentum-flow diagrams III through VII are shown in Fig. 31. These are the only momentum-flow diagrams representing the corresponding Feynman diagrams which contribute to the leading order. Each space-time amplitude is of the form

$$M \sim (-i)^{5n+6} g^{2n+3} \left(\frac{2p_{1+}}{\sqrt{2}}\right)^2 \left(\frac{-2p_{2-}}{\sqrt{2}}\right)^2 \left(\frac{-i}{2}\right)^n \prod_{j=1}^{n} \int \frac{d^2\vec{q}_{j\perp}}{(2\pi)^3} \prod_{k=1}^{n} \int dq_{k-} \frac{N}{D} \tag{5.31}$$

for some appropriate N and D.

Using the notation of Fig. 31(a) and assuming that $i \neq 1$, the dominant contribution to diagram III comes from the region

$$\frac{\lambda^2}{p_{1+}} \ll q_{n-} \ll \cdots \ll q_{i-} \ll k_- \ll q_{i-1-} \ll \cdots \ll q_{1-} \ll p_{2-}, \tag{5.32}$$

so that

$$q_{1+} = O\left(\frac{1}{p_{2-}}\right), \tag{5.33a}$$

$$q_{j+} \sim \frac{-c_{j-1}}{q_{j-1-}}, \quad j = 2, \ldots, i-1, i+1, \ldots, n \tag{5.33b}$$

and either

$$(1)\ q_{i+} \sim \frac{-c_{i-1}}{q_{i-1-}}$$

or (5.35)

$$(2)\ q_{i+} \sim \frac{-d_i}{k_- - q_{i-}},$$

where

$$d_j = (\vec{q}_{j\perp} - \vec{\Delta}_{2\perp})^2 + \lambda^2 . \tag{5.36}$$

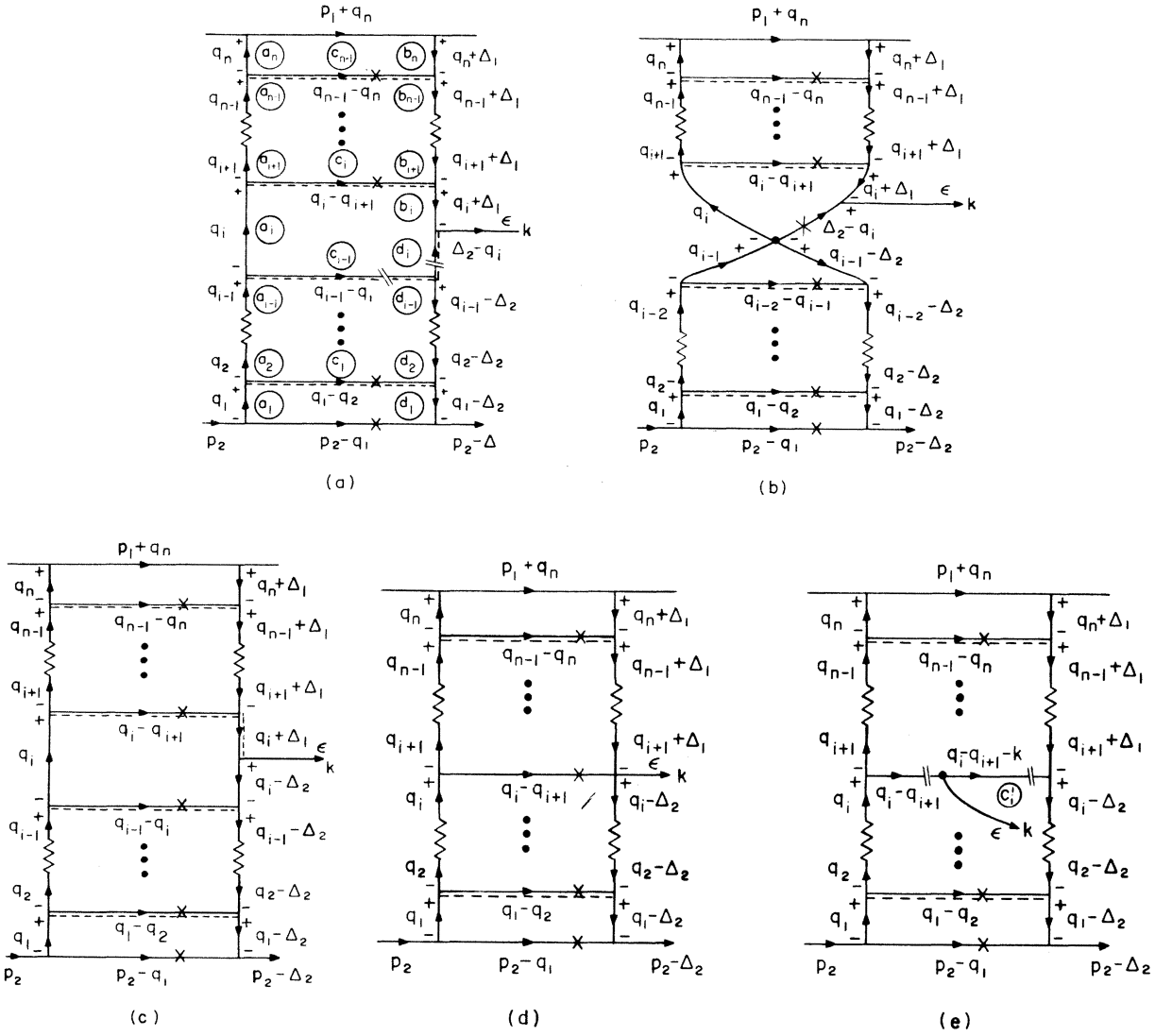

FIG. 31. Momentum-flow diagrams (a) III, (b) IV, (c) V, (d) VI, and (e) VII.

Let N_1 and D_1 (N_2 and D_2) be the numerator and denominator corresponding to the first (second) alternative for q_{i+}. Then

$$D_1 \sim -p_{1+}p_{2-}\left(\prod_{j=1}^{n} q_{j-}\right)\left(\prod_{k=1}^{n} a_k\right)\left(\prod_{l=i}^{n} b_l\right)\left(\prod_{m=1}^{i} d_m\right) \tag{5.37}$$

and

$$D_2 \sim p_{1+}p_{2-}q_{1-}\cdots q_{i-2-}(k_- - q_{i-})q_{i-}\cdots q_{n-}\left(\prod_{k=1}^{n} a_k\right)\left(\prod_{l=i}^{n} b_l\right)\left(\prod_{m=1}^{i-1} d_m\right)\left(\frac{q_{i-1-}}{k_- - q_{i-}} d_i - c_{i-1}\right), \tag{5.38}$$

so that to leading order $D_1 \sim -D_2$, and thus the numerator terms not proportional to q_{i+} cancel out.

It will be seen below that N_2 contains "large" terms which are $O(q_{i+}q_{i-1-} \sim q_{i-1-}/k_-)$ or $O(q_{i-}q_{i-1-}/k_-^2)$. These terms by themselves give a contribution much larger than n powers of logarithms of s_1 and s_2; however, they are exactly canceled by terms from flow diagram IV. Therefore, for the approximation scheme to be consistent (i.e., for $q_{j-} \ll p_{2-}$ to be the dominant region of integration), it is necessary to add together the contributions from diagrams III and IV, and likewise the contributions from diagrams V, VI, and VII, before performing the – momentum integrations. In diagram III, care must be taken to keep nonleading terms which are down by a factor of $1/q_{i+}q_{i-1-}$. In particular, this means that the polarization of the

line carrying momentum $\Delta_2 - q_i$ is arbitrary, although the polarization of all other vertical lines is still + at the top, − at the bottom.

The vertices which contribute terms proportional to q_{i+} are shown in Fig. 32. The vertex factor from Fig. 32(a) is

$$-\tfrac{1}{2}\vec{\epsilon}_\perp\cdot(4\vec{q}_{i\perp}+3\vec{\Delta}_{2\perp}-\vec{\Delta}_{1\perp})q_{i+}k_- -\vec{\epsilon}_\perp\cdot(\vec{\Delta}_{2\perp}-\vec{\Delta}_{1\perp}-2\vec{q}_{i\perp})q_{i+}q_{i-1-}-\epsilon_+k_-\left(\tfrac{1}{2}\,q_{i+}q_{i-1-}+\frac{1}{2}\,\frac{q_{i+}q_{i-}q_{i-1-}}{k_-}+\tfrac{1}{4}q_{i+}k_-\right)$$
$$+\tfrac{1}{2}\epsilon_-q_{i+}[(3\vec{q}_{i\perp}+\vec{\Delta}_{2\perp})\cdot(\vec{q}_{i\perp}+2\vec{\Delta}_{1\perp}+\vec{\Delta}_{2\perp})+(\vec{q}_{i-1\perp}+\vec{q}_{i\perp})\cdot(\vec{q}_{i-1\perp}+\vec{q}_{i\perp}-2\vec{\Delta}_{2\perp})]$$
$$-\tfrac{1}{4}\epsilon_-q_{i+}{}^2k_- +\tfrac{1}{4}\epsilon_-(k_+-q_{i+})(2q_{i+}q_{i-1-}+q_{i+}k_-)\,, \tag{5.39}$$

where terms not proportional to q_{i+} have been dropped. Its contribution to N_2, using (5.35), is

$$\left(\frac{q_{i-1-}}{k_- - q_{i-}}\,d_i - c_{i-1}\right)\left[\vec{\epsilon}_\perp\cdot(\vec{\Delta}_{2\perp}-\vec{\Delta}_{1\perp}-2\vec{q}_{i\perp})+\tfrac{1}{2}\epsilon_+(k_-+q_{i-})-\tfrac{1}{2}\epsilon_-\left(k_+ + \frac{d_i}{k_- - q_{i-}}\right)\right]$$
$$+c_{i-1}\left[\vec{\epsilon}_\perp\cdot(\vec{\Delta}_{2\perp}-\vec{\Delta}_{1\perp}-2\vec{q}_{i\perp})+\tfrac{1}{2}\epsilon_+k_- -\tfrac{1}{2}\epsilon_-\left(k_+ + \frac{d_i}{k_- - q_{i-}}\right)\right]$$
$$+\tfrac{1}{2}\vec{\epsilon}_\perp\cdot(4\vec{q}_{i\perp}+3\vec{\Delta}_{2\perp}-\vec{\Delta}_{1\perp})d_i+\tfrac{1}{4}\epsilon_+k_-d_i-\frac{1}{4}\,\frac{\epsilon_-}{k_-}\,d_i{}^2-\tfrac{1}{4}\epsilon_-\left(k_+\,\frac{d_i}{k_-}\right)d_i$$
$$-\frac{1}{2}\frac{\epsilon_-}{k_-}\,d_i((3\vec{q}_{i\perp}+\vec{\Delta}_{2\perp})\cdot(\vec{q}_{i\perp}+2\vec{\Delta}_{1\perp}+\vec{\Delta}_{2\perp})+(\vec{q}_{i-1\perp}+\vec{q}_{i\perp})\cdot(\vec{q}_{i-1\perp}+\vec{q}_{i\perp}-2\Delta_{2\perp}))\,. \tag{5.40}$$

The dominant contribution of momentum-flow diagram IV [Fig. 31(b)] again comes from the region (5.32) where (5.33) and (5.35) hold, and the denominator is

$$D_2\left(\frac{q_{i-1-}}{k_- - q_{i-}}\,d_i - c_{i-1}\right)^{-1}. \tag{5.41}$$

Using the Feynman rules given in Fig. 3, the four-vector vertex is the sum of two parts, one (called IVa) with the isospin of diagram III and the other with isospin similar to that of diagram III, but with the bottom horizontal line twisted. Each is proportional to

$$-\vec{\epsilon}_\perp\cdot(\vec{\Delta}_{2\perp}-\vec{\Delta}_{1\perp}-2\vec{q}_{i\perp})-\tfrac{1}{2}\epsilon_+(k_-+q_{i-})+\tfrac{1}{2}\epsilon_-\left(k_+ + \frac{d_i}{k_- - q_{i-}}\right). \tag{5.42}$$

Using (5.41), these terms precisely cancel the "large" terms from (5.40), as claimed above.

Using (5.34), the contribution of (5.39) to N_1 is

$$\vec{\epsilon}_\perp\cdot(\vec{\Delta}_{2\perp}-\vec{\Delta}_{1\perp}-2\vec{q}_{i\perp})c_{i-1}+\tfrac{1}{2}\epsilon_+k_-c_{i-1}-\tfrac{1}{2}\epsilon_-k_+c_{i-1}\,. \tag{5.43}$$

Since $D_1 \sim -D_2$, each of the terms in (5.43) cancels with a corresponding term in (5.40); so the sum of the contributions from (5.40), (5.42), and (5.43) is

$$\tfrac{1}{2}\vec{\epsilon}_\perp\cdot(4\vec{q}_{i\perp}+3\vec{\Delta}_{2\perp}-\vec{\Delta}_{1\perp})d_i+\tfrac{1}{4}\epsilon_+k_-d_i-\frac{1}{2}\frac{\epsilon_-}{k_-}d_i[c_{i-1}+d_i+\tfrac{1}{2}(\vec{k}_\perp{}^2+\lambda^2)+(3\vec{q}_{i\perp}+\vec{\Delta}_{2\perp})\cdot(\vec{q}_{i\perp}+2\vec{\Delta}_{1\perp}+\vec{\Delta}_{2\perp})$$
$$+(\vec{q}_{i-1\perp}+\vec{q}_{i\perp})\cdot(\vec{q}_{i-1\perp}+\vec{q}_{i\perp}-2\vec{\Delta}_{2\perp})]\,, \tag{5.44}$$

where the denominator is D_2. The term in brackets equals

$$3a_i+a_{i-1}+3b_i+d_{i-1}+\tfrac{3}{2}(\vec{k}_\perp{}^2+\lambda^2)-4(\vec{\Delta}_{1\perp}{}^2+\lambda^2)-3\lambda^2 \Rightarrow \tfrac{3}{2}(\vec{k}_\perp{}^2+\lambda^2)-4(\vec{\Delta}_{1\perp}{}^2+\lambda^2)-3\lambda^2\,, \tag{5.45}$$

where the divergent terms have been dropped.

The vertex contribution from Fig. 32 (b) is [using (5.35)]

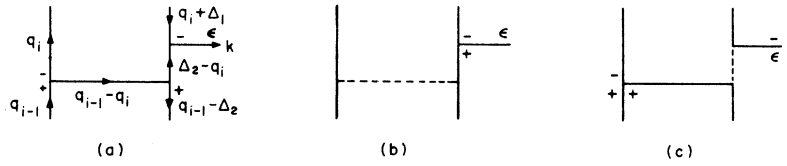

FIG. 32. Sections of momentum-flow diagram III.

$$-(-\lambda)^2(\epsilon_-/2k_-)d_i \tag{5.46}$$

and the contribution from Fig. 32(c) is

$$-2(-\lambda)^2(\epsilon_-/2k_-)d_i\,, \tag{5.47}$$

where the extra factor of 2 comes from the isospin amplitude, as will be shown below. Each of the upper $n-i$ rungs in flow diagrams III and IV contributes a factor of $2(\vec{\Delta}_{1\perp}^{\,2}+\lambda^2)$ and each of the lower $i-2$ rungs contributes a factor of $2(\vec{\Delta}_{2\perp}^{\,2}+\lambda^2)$. Therefore, from (5.31), (5.38), and (5.44) through (5.47),

$$M_{\mathrm{III}}+M^a_{\mathrm{IV}} \sim (-1)^{n+1}g^{2n+3}\frac{s}{(\vec{\Delta}_{1\perp}^{\,2}+\lambda^2)(\vec{\Delta}_{2\perp}^{\,2}+\lambda^2)}\frac{((\Delta_{1\perp}^{\,2}+\lambda^2)K_1\ln(s_1/\lambda^2))^{n-i+1}}{(n-i+1)!}\frac{((\vec{\Delta}_{2\perp}^{\,2}+\lambda^2)K_2\ln(s_2/\lambda^2))^{i-1}}{(i-1)!}$$
$$\times\left[\tfrac{3}{2}\vec{\epsilon}_\perp\cdot(\vec{\Delta}_{2\perp}-\vec{\Delta}_{1\perp})+\tfrac{1}{4}\epsilon_+k_-+\frac{\epsilon_-}{k_-}(-\tfrac{3}{4}(\vec{k}_\perp^{\,2}+\lambda^2)+2(\vec{\Delta}_{1\perp}^{\,2}+\lambda^2))\right]. \tag{5.48}$$

The isospin is that of diagram III.

If $i=1$, it is simple to show that

$$M_{\mathrm{III}}\sim(-1)^{n+1}g^{2n+3}s\frac{\ln^n(s_1/\lambda^2)}{n!}K_1{}^n(\vec{\Delta}_{1\perp}^{\,2}+\lambda^2)^{n-1}\frac{\epsilon_-}{k_-}\,. \tag{5.49}$$

Diagram IV does not contribute in this case.

As stated above, it is necessary to add the contributions from diagrams V, VI, and VII together in order to cancel out "large" terms. Using the notation of Fig. 31(c), and assuming that $i\neq n$, the dominant convergent contribution to flow diagram V comes from the region

$$\frac{\lambda^2}{p_{1+}}\ll q_{n-}\ll\cdots\ll q_{i+1-}\ll k_-\ll q_{i-}\ll\cdots\ll q_{1-}\ll p_{2-} \tag{5.50}$$

with the + momentum poles chosen to satisfy (5.33) and (5.34). Thus, using (5.31), the numerator and denominator are

$$D_3\sim p_{1+}p_{2-}\Big(\prod_{j=1}^{n}q_{j-}\Big)(k_+q_- - b_i)\Big(\prod_{l=1}^{n}a_l\Big)\Big(\prod_{m=1}^{i}d_m\Big)\Big(\prod_{p=i+1}^{n}b_p\Big)\,, \tag{5.51}$$

and

$$N_3\sim[2(\vec{\Delta}_{1\perp}^{\,2}+\lambda^2)]^{n-i-1}[2(\vec{\Delta}_2^{\,2}+\lambda^2)]^{i-1}\bar{N}_3\,, \tag{5.52}$$

where $\bar{N}_3$ is the sum of the factors from the vertices shown in Fig. 33. Since the large terms in $\bar{N}_3$ are $O(k_+{}^2q_{i-}{}^2)$, it is necessary to keep the next-to-leading terms of $O(k_+q_{i-})$, so that the polarization along the line carrying momentum $q_i+\Delta_1$ is arbitrary. The polarization of all other vertical lines is + at the top, − at the bottom. Summing over the polarizations, the contribution from Fig. 33(a) is

$$\tfrac{1}{2}q_{i-}k_+\vec{\epsilon}_\perp\cdot(4\vec{q}_{i\perp}-3\vec{\Delta}_{1\perp}+\vec{\Delta}_{2\perp})-\tfrac{1}{4}\epsilon_-k_+{}^2q_{i-}$$
$$+\tfrac{1}{2}\epsilon_+q_{i-}[(\vec{q}_{i\perp}-\vec{\Delta}_{1\perp}-2\vec{\Delta}_{2\perp})\cdot(3\vec{q}_{i\perp}-\vec{\Delta}_{1\perp})+(\vec{q}_{i\perp}+\vec{q}_{i+1\perp})\cdot(\vec{q}_{i\perp}+\vec{q}_{i+1\perp}+2\vec{\Delta}_{1\perp})]+\tfrac{1}{4}\epsilon_+(2q_{i-}{}^2k_+-2q_{i-}{}^2q_{i+1+}+q_{i-}k_-k_+)$$
$$=\tfrac{1}{2}q_{i-}k_+\vec{\epsilon}_\perp\cdot(4\vec{q}_{i\perp}-3\vec{\Delta}_{1\perp}+\vec{\Delta}_{2\perp})-\tfrac{1}{4}\epsilon_-k_+{}^2q_{i-}+\tfrac{1}{2}\epsilon_+q_{i-}(q_{i-}k_+-b_i)$$
$$+\tfrac{1}{2}\epsilon_+q_{i-}(3a_i+a_{i+1}+b_{i+1}+3d_i+\tfrac{3}{2}(\vec{k}_\perp^{\,2}+\lambda^2)-4(\vec{\Delta}_{2\perp}^{\,2}+\lambda^2)-3\lambda^2)\,. \tag{5.53}$$

The contributions from Figs. 33(b) and 33(c) are

$$-(-\lambda)^2(-\tfrac{1}{2}\epsilon_+q_{i-}) \tag{5.54}$$

and

$$-2(-\lambda)^2(-\tfrac{1}{2}\epsilon_+q_{i-})\,, \tag{5.55}$$

respectively, where the extra factor of 2 in (5.55) is due to the isospin and will be justified below. Therefore, from (5.53), (5.54), and (5.55), dropping divergent terms,

$$\bar{N}_3\sim\tfrac{1}{2}q_{i-}k_+\Big(\vec{\epsilon}_\perp\cdot(4\vec{q}_{i\perp}-3\vec{\Delta}_{1\perp}+\vec{\Delta}_{2\perp})-\tfrac{1}{2}\epsilon_-k_++\frac{\epsilon_+}{k_+}(q_{i-}k_+-b_i)+\frac{\epsilon_+}{k_+}(\tfrac{3}{2}(\vec{k}_\perp^{\,2}+\lambda^2)-4(\vec{\Delta}_{2\perp}^{\,2}+\lambda^2))\Big)\,. \tag{5.56}$$

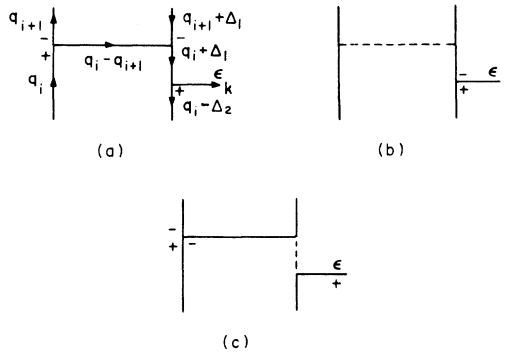

FIG. 33. Sections of momentum-flow diagram V.

For momentum-flow diagram VI in Fig. 31(d), (5.31), (5.33), (5.34), and (5.50) still hold, with numerator and denominator

$$D_4 \sim D_3(k_+ q_{i-} - b_i)^{-1} \tag{5.57}$$

and

$$N_4 = [2(\vec{\Delta}_{1\perp}^{\,2} + \lambda^2)]^{n-i-1}[2(\vec{\Delta}_{2\perp}^{\,2} + \lambda^2)]^{i-1}\bar{N}_4 . \tag{5.58}$$

$\bar{N}_4$ consists of several terms, illustrated diagrammatically in Fig. 34. In Fig. 34(a) each of the two terms has the isospin of diagram V (this will be seen below), and in Fig. 34(b) one term has the isospin of diagram VII and the other has the isospin of diagram V. This last cancels with the large term in (5.56).

Figure 31(e) shows momentum-flow diagram VII. The other flow diagrams corresponding to this Feynman diagram give no net contribution. The region of integration is still (5.50) with

$$q_{1+} = O\left(\frac{1}{p_{2-}}\right), \tag{5.59a}$$

$$q_{j+} \sim \frac{-c_{j-1}}{q_{j-1-}}, \quad j = 1, \ldots, i, i+2, \ldots, n \tag{5.59b}$$

and either

$$\text{(a)}\quad q_{i+1+} \sim \frac{-c_i}{q_{i-}} \tag{5.60}$$

or

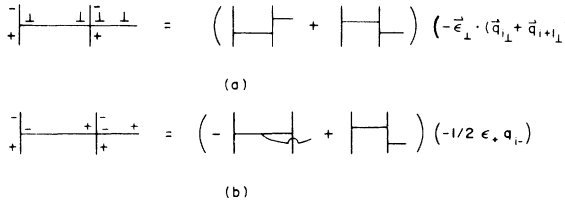

FIG. 34. Numerator and isospin factors from momentum-flow diagram VI. The isospin is represented diagrammatically.

$$\text{(b)}\quad q_{i+1+} \sim -k_+ - \frac{c_i'}{q_{i-} - k_-}, \tag{5.61}$$

where

$$c_i' = (\vec{q}_{i\perp} - \vec{q}_{i+1\perp} - \vec{\Delta}_{1\perp} - \vec{\Delta}_{2\perp})^2 + \lambda^2 . \tag{5.62}$$

The corresponding denominators are

$$D_a \sim p_{1+}p_{2-}\left(\prod_{j=1}^{n} q_{j-}\right)\left(\prod_{k=1}^{n} a_k\right)\left(\prod_{l=i+1}^{n} b_l\right)\left(\prod_{m=1}^{i} d_m\right) \times (-q_{i-}k_+ + c_i - c_i' + \vec{k}_\perp^{\,2} + \lambda^2) \tag{5.63}$$

and

$$D_b \sim p_{1+}p_{2-}q_{1-}\cdots q_{i-1-}(q_{i-} - k_-)q_{i+1-}\cdots q_{n-} \times \left(\prod_{k=1}^{n} a_k\right)\left(\prod_{l=i+1}^{n} b_l\right)\left(\prod_{m=1}^{i} d_m\right)(k_+ q_{i-} + c_i' - c_i) . \tag{5.64}$$

Since

$$(q_{i-} - k_-)(k_+ q_{i-} + c_i' - c_i) \sim q_{i-}(k_+ q_{i-} + c_i' - c_i - (\vec{k}^2 + \lambda^2)), \tag{5.65}$$

$D_a \sim -D_b$ to leading and next-to-leading powers of k_-/q_{i-}. Because of this and since the numerator contains large terms of $O(k_+^{\,2} q_{i-}^{\,2})$, numerator terms not proportional to q_{i+1+} cancel out:

$$N_a = [2(\vec{\Delta}_{1\perp}^{\,2} + \lambda^2)]^{n-i-1}[2(\vec{\Delta}_{2\perp}^{\,2} + \lambda^2)]^{i-1}\bar{N}_a , \tag{5.66}$$

and likewise for N_b, where $\bar{N}_a$ and $\bar{N}_b$ are determined from the three vertices on the horizontal line in the middle of Fig. 31(e). Each is of the form

$$-\vec{\epsilon}_\perp \cdot (2\vec{q}_{i\perp} - 2\vec{q}_{i+1\perp} - \vec{\Delta}_{1\perp} - \vec{\Delta}_{2\perp})q_{i-}q_{i+1+} - \epsilon_- q_{i-}(q_{i+1+}^{\,2} + q_{i+1+}k_+) + \epsilon_+ q_{i-}q_{i+1+}(q_{i-} - k_-) . \tag{5.67}$$

Since

$$\int d^2\vec{q}_\perp \frac{\vec{q}_\perp}{(\vec{q}_\perp^{\,2} + \lambda^2)((\vec{q}_\perp + \vec{\Delta}_\perp)^2 + \lambda^2)} = \int d^2\vec{q}_\perp \frac{-\frac{1}{2}\vec{\Delta}_\perp}{(\vec{q}_\perp^{\,2} + \lambda^2)((\vec{q}_\perp + \vec{\Delta}_\perp)^2 + \lambda^2)} \tag{5.68}$$

one can make the replacements $\vec{q}_{i+1\perp} \to -\frac{1}{2}\vec{\Delta}_{1\perp}$ and $\vec{q}_{i\perp} \to \frac{1}{2}\vec{\Delta}_{2\perp}$ in (5.67); thus there is no net $\epsilon_\perp$ component. The ϵ_- component also drops out and

$$\bar{N}_a \sim -\epsilon_+ q_{i-}c_i , \tag{5.69}$$

$$\bar{N}_b \sim -\epsilon_+ q_{i-}(k_+ q_{i-} + c_i' - c_i - (\vec{k}_\perp^{\,2} + \lambda^2)) - \epsilon_+ q_{i-} c_i , \tag{5.70}$$

so that

$$\frac{\bar{N}_a}{D_a} + \frac{\bar{N}_b}{D_b} \sim \frac{-\epsilon_+ q_{i-}}{D_4} . \tag{5.71}$$

Therefore, from (5.31), (5.50), (5.51), (5.52), (5.56), (5.57), (5.58), (5.66), and (5.71),

$$M_V + M_{VI} + \tfrac{1}{2} M_{VIII} \sim (-1)^{n+1} g^{2n+3} S \frac{1}{(\vec{\Delta}_{1\perp}^{\,2} + \lambda)(\vec{\Delta}_{2\perp}^{\,2} + \lambda^2)} \frac{((\vec{\Delta}_{1\perp}^{\,2} + \lambda^2) K_1 \ln(s_1/\lambda^2))^{n-i}}{(n-i)!} \frac{((\vec{\Delta}_{2\perp}^{\,2} + \lambda^2) K_2 \ln(s_2/\lambda^2))^{i}}{i!}$$
$$\times \left[\tfrac{1}{2} \vec{\epsilon}_\perp \cdot (\vec{\Delta}_{2\perp} - \vec{\Delta}_{1\perp}) - \tfrac{1}{4} \epsilon_- k_+ + \frac{\epsilon_+}{k_+} \left(\tfrac{3}{4} (\vec{k}_\perp^{\,2} + \lambda^2) - 2(\vec{\Delta}_{2\perp}^{\,2} + \lambda^2) \right) \right] , \tag{5.72}$$

where the isospin is that of diagram V.

If $i = n$, only diagram V contributes, and

$$M_V \sim (-1)^n g^{2n+3} S \frac{\ln^n(s_2/\lambda^2)}{n!} K_2^{\,n} (\vec{\Delta}_{2\perp}^{\,2} + \lambda^2)^{n-1} \frac{\epsilon_+}{k_+} . \tag{5.73}$$

The Feynman diagrams formed from diagrams IV through VII by twisting the top horizontal line, by twisting the bottom horizontal line, or by twisting both the top and bottom horizontal lines also contribute to the scattering amplitude. For each of diagrams IV and VII this procedure produces only one, instead of three, new distinct Feynman diagrams. To compensate for this, the amplitude of diagram VII is multiplied by $\frac{1}{2}$ [as in (5.72)]; then each of the four diagrams must be considered. In the case of diagram IV, it was shown above that in the high-energy limit, the amplitude is the sum of two terms with different isospin factors, one being obtained from the other by twisting the bottom horizontal line. So in this sense there are three new "diagrams" formed by applying the above procedure to that part of Feynman diagram III used in computing (5.48).

Comparing propagators on the high-momentum lines shows that the sum of the space-time amplitudes of the Feynman diagrams formed by twisting the bottom (top) horizontal lines equals minus the sum of the space-time amplitudes of the original Feynman diagrams [i.e., (5.48) plus (5.72)], and, similarly, twisting both lines reproduces the original amplitude. This is true because (5.48) and (5.72) contain no net contribution from large terms, so that $q_{j-} \ll p_{2-}$ is a valid approximation, and equations such as (3.12) hold. Note that this is not true for individual Feynman diagrams; for example, the space-time amplitudes corresponding to the two different isospin factors of diagram III are equal, not negatives of each other.

The combined isospin of all these diagrams is calculated in Fig. 35 and equals $I_1^{(3)}$. Use is made of Figs. 8 and 12 and the identity $(i\epsilon_{cad})(i\epsilon_{cdb}) = 2\delta_{ab}$, illustrated diagrammatically in Fig. 35(c). Figure 35(b) justifies the extra factor of 2 in (5.47) and (5.55). Consequently, from (5.48), (5.49), (5.72), and (5.73), the amplitude of diagrams III through VII is

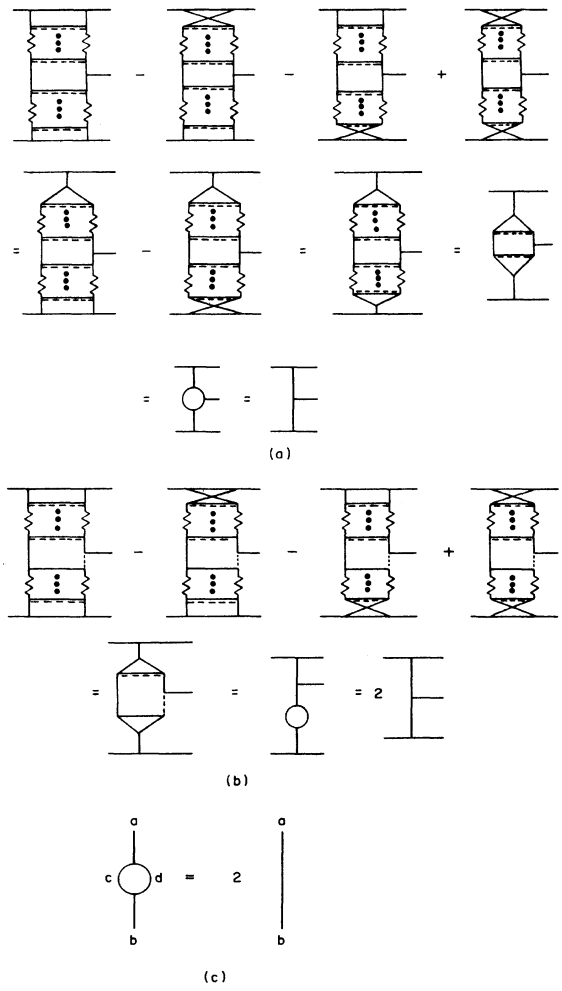

FIG. 35. (a), (b) The isospin calculation for diagrams III through VII. (c) The isospin identity $(i\epsilon_{cad})(i\epsilon_{cdb}) = 2\delta_{ab}$.

$$\mathfrak{M}_{\mathrm{III}\to\mathrm{VII}} \sim (-1)^{n+1} g^{2n+3} s \left[\frac{\ln^n(s_1/\lambda^2)}{n!} K_1{}^n (\vec{\Delta}_{1\perp}{}^2+\lambda^2)^{n-1} \frac{\epsilon_-}{k_-} - \frac{\ln^n(s_2/\lambda^2)}{n!} K_2{}^n (\vec{\Delta}_{2\perp}{}^2+\lambda^2)^{n-1} \frac{\epsilon_+}{k_+} \right] I_1^{(3)}$$
$$+ (-1)^n g^{2n+3} \frac{2s}{(\vec{\Delta}_{1\perp}{}^2+\lambda^2)(\vec{\Delta}_{2\perp}{}^2+\lambda^2)} \left[\vec{\epsilon}_\perp \cdot (\vec{\Delta}_{1\perp} - \vec{\Delta}_{2\perp}) - \epsilon_+ k_- \left(\frac{1}{2} - \frac{\vec{\Delta}_{2\perp}{}^2+\lambda^2}{\vec{k}_\perp{}^2+\lambda^2} \right) + \epsilon_- k_+ \left(\frac{1}{2} - \frac{\vec{\Delta}_{1\perp}{}^2+\lambda^2}{\vec{k}_\perp{}^2+\lambda^2} \right) \right]$$
$$\times \frac{1}{n!} \sum_{i=1}^{n-1} \binom{n}{i} \left((\vec{\Delta}_{1\perp}{}^2+\lambda^2) K_1 \ln \frac{s_1}{\lambda^2} \right)^{n-i} \left((\vec{\Delta}_{2\perp}{}^2+\lambda^2) K_2 \ln \frac{s_2}{\lambda^2} \right)^i I_1^{(3)} . \tag{5.74}$$

From (5.14), (5.19), (5.27), (5.28), (5.29), (5.30), and (5.74), the total amplitude for n loops is

$$\mathfrak{M} \sim g^3 \frac{2s}{(\vec{\Delta}_{1\perp}{}^2+\lambda^2)(\vec{\Delta}_{2\perp}{}^2+\lambda^2)} \left[\vec{\epsilon}_\perp \cdot (\vec{\Delta}_{1\perp} - \vec{\Delta}_{2\perp}) - \epsilon_+ k_- \left(\frac{1}{2} - \frac{\vec{\Delta}_{2\perp}{}^2+\lambda^2}{\vec{k}_\perp{}^2+\lambda^2} \right) + \epsilon_- k_+ \left(\frac{1}{2} - \frac{\vec{\Delta}_{1\perp}{}^2+\lambda^2}{\vec{k}_\perp{}^2+\lambda^2} \right) \right]$$
$$\times \frac{1}{n!} \left[-g^2 (\vec{\Delta}_{1\perp}{}^2+\lambda^2) K_1 \ln\left(\frac{s_1}{\lambda^2}\right) - g^2 (\vec{\Delta}_{2\perp}{}^2+\lambda^2) K_2 \ln\left(\frac{s_2}{\lambda^2}\right) \right]^n I_1^{(3)} , \tag{5.75}$$

which is the $(n+1)$st term in the power-series expansion of (1.1).

A similar analysis shows that the amplitude for scalar production comes from momentum-flow diagrams analogous to flow diagrams II through V, where the created vector particle is replaced by a scalar. The space-time amplitudes of diagrams II, III plus IV, and V are respectively

$$(-1)^n g^{2n+3} s \frac{\ln^n(s_1/\lambda^2)}{n!} K_1{}^n \frac{(\vec{\Delta}_{1\perp}{}^2+\lambda^2)^{n-1}}{(\vec{\Delta}_{2\perp}{}^2+\lambda^2)} (-\lambda) , \tag{5.76}$$

$$(-1)^n g^{2n+3} \frac{\frac{1}{2}s}{(\vec{\Delta}_{1\perp}{}^2+\lambda^2)(\vec{\Delta}_{2\perp}{}^2+\lambda^2)} \frac{((\vec{\Delta}_{1\perp}{}^2+\lambda^2) K_1 \ln(s_1/\lambda^2))^{n-i+1}}{(n-i+1)!} \frac{((\vec{\Delta}_{2\perp}{}^2+\lambda^2) K_2 \ln(s_2/\lambda^2))^{i-1}}{(i-1)!} (-\lambda) , \quad i>1 \tag{5.77}$$

and

$$(-1)^n g^{2n+3} \frac{\frac{1}{2}s}{(\vec{\Delta}_{1\perp}{}^2+\lambda^2)(\vec{\Delta}_{2\perp}{}^2+\lambda^2)} \frac{((\vec{\Delta}_{1\perp}{}^2+\lambda^2) K_1 \ln(s_1/\lambda^2))^{n-i}}{(n-i)!} \frac{((\vec{\Delta}_{2\perp}{}^2+\lambda^2) K_2 \ln(s_2/\lambda^2))^{i}}{i!} (-\lambda) , \quad i<n . \tag{5.78}$$

The diagram formed by reflecting the scalar production version of diagram II through a horizontal plane mirror also contributes and its amplitude is obtained from (5.76) by the transformation (2.11). The combined isospin of these diagrams and those formed by twisting the top and bottom horizontal lines is twice that of the diagram in Fig. 2(b). The sum of the amplitudes then reproduces the $(n+1)$st term in the power-series expansion of (1.1).

VI. CONCLUSIONS

This result of Reggeization in a Yang-Mills theory contrasts with those in quantum electrodynamics (QED) and in ϕ^3 theory. In both QED and ϕ^3 the lowest-order terms (from the Born diagram for elastic scattering and the tree diagrams for inelastic scattering) are predominantly real, whereas the sum of the ladder and the crossed-ladder diagrams and the sum of the corresponding diagrams for production processes are predominantly imaginary. These diagrams do not add together as they do in Yang-Mills theory, where the leading amplitudes are real. Thus the Regge-pole form in the elastic channel of ϕ^3 theory, for example, comes from summing over the ladder and crossed-ladder diagrams only, and the analogous situation holds for the inelastic channels.[16] Further, for two-body-to-three-body processes in ϕ^3 theory, if

$$\eta = \frac{s}{s_1 s_2} \sim \frac{1}{\vec{k}^2+\lambda^2} ,$$

where $\vec{k}$ is the transverse momentum of the produced particle, then the scattering amplitude has a branch point in the complex η plane; in Yang-Mills theory, the amplitude is an entire function of η.

The result of this paper also lends support to the calculation of Fadin, Kuraev, and Lipatov[7] of the elastic amplitude in Yang-Mills theory. Their conclusion was that in the leading-logarithm approximation, the Froissart bound[17] is violated.[18] In order to calculate the elastic amplitude via their unitarity approach, it is necessary to know the inelastic amplitudes for two particles going into n particles, $2\to n$. Based on the Reggeized form of the vector meson for the $2\to 2$ amplitude, those authors used a multi-Regge-pole form for

all the inelastic processes. The present paper explicitly verifies that this form is correct for $2 \to 3$ scattering. It would be interesting to determine whether the amplitude for $2 \to 4$, or indeed for $2 \to n$, is also of the Regge-pole form. If so, this means that the cross section for production of n particles decreases rapidly with increasing energy, so that the violation of the Froissart bound is due to the increasing number of open channels. It would further be interesting to determine whether, in the leading-logarithm approximation, the inelastic amplitudes also violate unitarity.

ACKNOWLEDGMENT

I sincerely thank Professor Hung Cheng for his encouragement, benevolence, and essential comments.

APPENDIX

Here it is demonstrated that the polarization along all vertical lines of Feynman diagram I is + at the top and − at the bottom. Associate a number with each vertex Γ as follows: Make the assignment

$$+ \to +1,$$

$$\perp \to 0,$$

$$- \to -1$$

and define $N(\Gamma)$ to be the sum of the numbers corresponding to the three polarizations associated with Γ. From the Feynman rule for a three-vector vertex, given in Fig. 3, each vertex is proportional to a four-vector with +, $\perp$, or − polarization if and only if $N(\Gamma)$ is +1, 0, or −1, respectively. Let the vertices be numbered so that Γ_1 and Γ_2 are on the top horizontal "rung," just below the large + momentum line, Γ_3 and Γ_4 are on the next lower rung, and so on down to Γ_{2m-1} and Γ_{2m} on the mth and lowest rung. Then, since the polarization of the lines emerging from the high-momentum line is + at the top, − at the bottom, and since the sum of the two numbers assigned to the polarizations on either end of any line is zero, it follows that $\sum_{i=1}^{2j} N(\Gamma_i) \leq 0$ for all $j \leq m$, and that $\sum_{i=1}^{2m} N(\Gamma_i) = 0$. From (5.6) and (5.7) $q_{i-} \gg q_{j-}$ if $i < j$, and $q_{i+} = O(1/q_{i-1,-})$, so the largest value of the numerator factor $\Gamma_1 \cdots \Gamma_{2m}$ is obtained if $N(\Gamma_{2i-1}) + N(\Gamma_{2i}) = 0$ for all i. This is only possible if the polarization of all the vertical lines is + at the top, − at the bottom. This argument can be modified to deal with other Feynman diagrams.

---

[1] M. T. Grisaru, H. J. Schnitzer, and H.-S. Tsao, Phys. Rev. Lett. 30, 811 (1973); Phys. Rev. D 8, 4498 (1973).

[2] B. M. McCoy and T. T. Wu, Phys. Rev. D 12, 3257 (1975); 13, 1076 (1976).

[3] L. N. Lipatov, Yad. Fiz. 23, 642 (1976) [Sov. J. Nucl. Phys. 23, 338 (1976)].

[4] H. Cheng and C. Y. Lo, Phys. Rev. D 15, 2959 (1977).

[5] P. W. Higgs, Phys. Lett. 12, 132 (1964); Phys. Rev. Lett. 13, 508 (1964); F. Englert and R. Brout, *ibid.* 13, 321 (1964); G. S. Guralnik, C. R. Hagen, and T. W. B. Kibble, *ibid.* 13, 585 (1964).

[6] L. D. Faddeev and V. N. Popov, Phys. Lett. 25B, 29 (1967).

[7] V. S. Fadin, E. A. Kuraev, and L. N. Lipatov, Phys. Lett. 60B, 50 (1975).

[8] For a discussion of the infinite-momentum-space technique, see H. Cheng and T. T. Wu, Phys. Rev. 182, 1899 (1969).

[9] For the Feynman rules, see G. 't Hooft and M. Veltman, in *Renormalization of Yang-Mills Fields and Applications to Particle Physics*, Marseille, France, 1972, edited by C. P. Korthals-Altes (C.N.R.S., Marseille, France, 1972).

[10] In the high-energy limit, with bounded mometum transfer, where the high-momentum particles are transversely polarized, there are no contributing diagrams where each line emanating from a vertex carries large momentum. For example, for each three-point vertex with large + momentum passing through it, there are two lines with large + momentum and one line with much smaller + momentum (which is said to "emerge" from the large momentum line). Thus it is possible to distinguish a single line which carries large + momentum and a (distinct) single line which carries large − momentum. The convention used here in drawing Feynman diagrams is that the large + (−) momentum line is the horizontal line at the top (bottom) of the graph.

[11] If $(F_a)_{bc} = i\epsilon_{abc}$, then the Jacobi identity is $[F_a, F_b] = -i\epsilon_{abc}F_c$.

[12] A more careful analysis shows that there are regions of width $O(1/p_{1+})$ which have been lost by approximating D_1 as in (3.3). However, these regions do not contribute to leading order.

[13] This argument only shows that the largest terms cancel; it does not prove that the remaining contribution is smaller than the terms kept from other diagrams. A direct calculation does indeed show it to be so.

[14] It is always possible to express the divergent integrals that appear in the calculation in a unique way as the sum of a convergent part and a divergent part. Confer the fifth-order calculation.

[15] For a reference on momentum-flow diagrams, see B. M. McCoy and T. T. Wu, Phys. Rev. D 13, 379 (1976).

[16] J. C. Polkinghorne, Nuovo Cimento 36, 857 (1965).

[17] M. Froissart, Phys. Rev. 123, 1053 (1961).

[18] This result was also obtained by Cheng and Lo (see Ref. 4), who used a different approach.